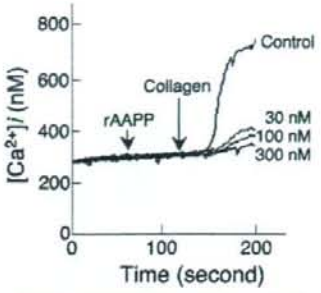

Figure 6. Effect of AAPP on $[Ca^{2+}]i$ in the early phase of collagen stimulation. Fura-2 AM-loaded platelets were incubated with 1 mM $CaCl_2$ for 5 minutes. Collagen (0.5 μg/mL) was added after a 60-second incubation with rAAPP (30, 100 or 300 nM), and the fura-2 fluorescence was determined. Tracings are representative results of a typical experiment.

AAPP inhibits the collagen-induced increase in $[Ca^{2+}]i$

Because an increase in $[Ca^{2+}]i$ is considered to play a pivotal role in platelet aggregation, we investigated the possible involvement of AAPP in the regulation of $[Ca^{2+}]i$. Addition of collagen to a human platelet suspension in the presence of 1 mM $CaCl_2$ resulted in an increase in $[Ca^{2+}]i$ (Figure 6 control). To determine the effects of AAPP on the collagen-induced increase in $[Ca^{2+}]i$, platelets were incubated with various concentrations of rAAPP for 1 minute before their activation with collagen. Even at a low concentration (30 nM), rAAPP drastically decreased the collagen-induced change in $[Ca^{2+}]i$, and 300 nM rAAPP completely abolished the change (Figure 6).

Intravenous administration of AAPP inhibits collagen-induced platelet aggregation ex vivo in rats

rAAPP also exhibited identical inhibition of collagen-induced aggregation of rat platelets in vitro (data not shown). The in vivo effects of rAAPP were tested by giving SD rats a bolus intravenous injection of rAAPP (0.1-1.0 mg/kg) and performing ex vivo aggregation studies on citrated PRP. The ED_{50} for the aggregation inhibition was 0.3 mg/kg, and rAAPP at 1.0 mg/kg prevented all detectable collagen-induced platelet aggregation (Figure 7). ADP-induced aggregation remained unaltered, even as concentrations as high as 1.0 mg/kg. There was no significant change in platelet aggregation after rTrx injection, which was used as a negative control.

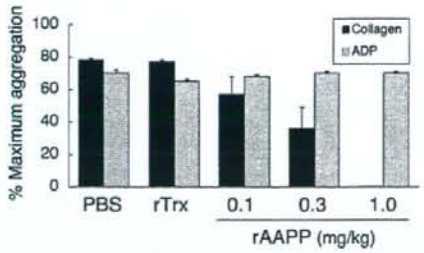

Figure 7. Inhibition of ex vivo collagen-induced aggregation of rat platelets after injection of AAPP. SD rats were administered rAAPP (0.1, 0.3, or 1.0 mg/kg) intravenously, and blood was drawn 10 minutes after the administration. Treatment with rAAPP results in inhibition of platelet aggregation in response to collagen, compared with treatment with PBS and rTrx, but has no effect on the ADP response. Results are means plus or minus SEM for 3 animals in each group.

Discussion

In the present study, we have identified and characterized an abundant saliva protein, AAPP, from the *A stephensi* mosquito. AAPP has characteristic features of acidic secreted proteins with a glycine and glutamic acid-rich region, and is specifically expressed in the distal lateral lobes of the adult female salivary glands. This expression pattern is consistent with the finding in our previous study on transgenic mosquitoes that the strong *aapp* promoter specifically drives foreign gene expression in the distal lateral lobes.[11] We have demonstrated that AAPP is unique in that it specifically blocks platelet adhesion to collagen and subsequent platelet aggregation.

Regarding the mechanism by which AAPP specifically inhibits collagen-induced platelet aggregation, AAPP directly binds to collagen I and III, and interferes with the interaction between collagen and its receptor GPVI on platelets, thereby inhibiting an increase in $[Ca^{2+}]i$, which is an important second messenger in the platelet activation cascade. The current view of collagen-induced platelet activation is that collagen initially interacts with GPVI and integrin $\alpha_2\beta_1$, and platelet activation signals are then conveyed by GPVI (reviewed in Nieswandt and Watson[36]). However, we excluded the possibility of direct interactions between AAPP and these molecules by the following pieces of evidence: (1) the 2 GPVI receptor agonists, CRP and convulxin did not compete with AAPP for platelet aggregation; (2) GPVI-expressing Jurkat cells did not bind to AAPP; and (3) the sequence motifs of the specific $\alpha_2\beta_1$ ligand, GFOGER-GPP,[37] within the collagen triple-helical region and the RGD fibrinogen receptor antagonist were not contained in the AAPP sequence. Our recent investigations have shown that, although the GE-rich region located in the N-terminal half of AAPP shows 65% similarity with the triple-helix region of the α-1 chain of human collagen IV (Figure S1B), this region is involved in the binding neither to GPVI (Figure 5E) nor collagen (S.Y. and T.S., unpublished data, July 2005). Further studies are currently in progress to identify AAPP receptor on collagen by using truncated rAAPPs.

To develop new therapeutic agents for the treatment of cardiovascular and ischemic disorders, a number of new exogenous factors have recently been identified from animal sources, and the search is still on for novel factors that interfere with platelet aggregation and blood coagulation (reviewed in Kini[38]). Although some factors effectively affect platelet function and aggregation in vitro, most of them fail to retain their biochemical and pharmacologic characteristics in vivo. To date, limited numbers of drugs have been developed or are in the process of being developed from animal sources, for example, desmoteplase (a plasminogen activator) from vampire bat saliva,[39-41] calin (a plasminogen activator) from *Hirudo medicinalis* leech saliva[42,43]; and hirudin (an anticoagulant) from *H medicinalis* leech saliva.[44,45] Our finding that intravenously administered rAAPP strongly inhibited collagen-mediated platelet aggregation ex vivo in rats may provide a potential use of AAPP for developing new drugs that maintain the flow of blood.

Malaria transmitted by anopheline mosquitoes is the worst health problem in the world, and kills 1 to 2 million people every year. Our recent studies on malaria survey have shown that approximately 90% of people living in the Solomon Islands, where malaria is hyperendemic, have high levels of antibodies against AAPP and the antibody levels are positively correlated with the antibody levels against malaria antigens (data not shown). From the

Direct binding of AAPP to collagen interferes with adhesion of platelets to collagen

When rAAPP was incubated with immobilized collagen in a 96-well plate, rAAPP effectively bound to collagen in a dose-dependent manner (Figure 3C). Moreover, the rAAPP binding strongly interfered with adhesion of platelets to the immobilized collagen in a dose-dependent manner (Figure 3D). The IC_{50} of the platelet adhesion blocking was 250 nM, and 1000 nM rAAPP completely prevented detectable platelet adhesion to collagen. Next, we examined the possible involvement of AAPP in interactions with GPVI. Figure 3E shows that GPVI-expressing Jurkat cells bound to collagen type I–coated plate, but not to AAPP-coated plate, indicating that AAPP dose not involved in direct interaction with GPVI. This result is consistent with the data that rAAPP had no effect on 2 GPVI agonists (Figure 3A).

AAPP acts as an antagonist of receptors that mediate adhesion of platelets to collagen

We found that the AAPP-mediated platelet aggregation inhibition is due to interfere with collagen-platelet interaction by direct binding of AAPP to collagen. Collagen induces platelet aggregation by interacting with GPVI[24,25] and integrin $\alpha_2\beta_1$[30,31] on the surface of platelets. GPVI- and integrin $\alpha_2\beta_1$-mediated platelet adhesion are well characterized. Integrin $\alpha_2\beta_1$ is known to mediate platelet adhesion to collagen in a Mg^{2+}-dependent manner.[32] Human platelets adhere to soluble monomeric collagen in a Mg^{2+}-dependent manner, while they adhere to insoluble polymeric collagen in a Mg^{2+}-independent manner.[33] The studies with anti-integrin $\alpha_2\beta_1$ and anti-GPVI antibodies indicate that integrin $\alpha_2\beta_1$ mediates the platelet adhesion to soluble monomeric collagen in a Mg^{2+}-dependent manner,[22,34,35] and that GPVI mediates the platelet adhesion to insoluble fibrillar collagen in a Mg^{2+}-independent manner.[22] Therefore, to address whether AAPP interferes with platelet adhesion by selectively binding to collagen receptors, we examined the effects of AAPP on platelet adhesion to soluble collagen in the presence of Mg^{2+} (integrin $\alpha_2\beta_1$-mediation) and to insoluble collagen in the absence of Mg^{2+} (GPVI-mediation). Various concentrations of rAAPP were incubated with insoluble fibrillar type I collagen immobilized in a 96-well plate before adding platelet suspension under static conditions in the absence of Mg^{2+}. Figure 4A shows that GPVI-mediated platelet adhesion was abolished by increasing amounts of rAAPP. The IC_{50} was approximately 22 nM, and complete inhibition was reached with 222 nM (10 μg/mL). As a positive control, a mouse mAb specific for human GPVI, OM-2 (1 μg/mL), strongly inhibited the platelet adhesion (> 95%). Next, we examined the ability of rAAPP on the binding of integrin $\alpha_2\beta_1$ under static conditions. In the presence of Mg^{2+}, integrin $\alpha_2\beta_1$-mediated platelet adhesion to nonfibrillar type I collagen was reduced by increasing amounts of rAAPP (IC_{50}≈222 nM) (Figure 4B). As a positive control, a mouse mAb specific for human integrin α_2-subunit, 6F1 (5 μg/mL), strongly inhibited the platelet adhesion (> 95%). Thus, AAPP effectively inhibited both GPVI- and integrin $\alpha_2\beta_1$-mediated platelet adhesion to collagen.

AAPP inhibits GPVI-mediated platelet adhesion to collagen type I, III, but not type IV

Because different types of collagen are among the most thrombogenic component of the vessel wall responsible for the initiation of platelet adhesion, we examined the ability of rAAPP to bind to these collagens. Various concentrations of rAAPP were incubated either with collagen type I, III or IV immobilized in a 96-well plate.

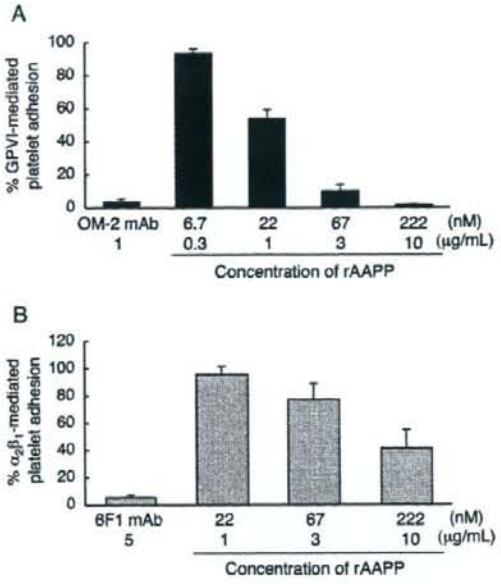

Figure 4. AAPP inhibits both GPVI- and integrin $\alpha_2\beta_1$-mediated platelet adhesion to collagen. The indicated concentrations of rAAPP were incubated in 96-well plates coated with fibrillar type I collagen in the absence of Mg^{2+} (A) or with nonfibrillar type I collagen in the presence of Mg^{2+} (B) for 1 hour. After washing, washed platelet suspensions were allowed to adhere under static conditions to each well for 1 hour. After washing, adhesion platelets were quantified fluorometrically. As positive controls, washed platelet suspension were preincubated with antihuman GPVI mAb, OM-2 (1 μg/mL) (A) or anti-(human integrin α_2-subunit) mAb, 6F1 (5 μg/mL) (B). Results are representative of 3 independent experiments and expressed as the mean of triplicate reading plus or minus SEM for the indicated concentrations.

The binding of rAAPP to each collagen was evaluated by studying the inhibition of GPVI-expressing Jurkat cells to binding to each collagen. Figure 5 shows that rAAPP inhibited the binding of GPVI-expressing Jurkat cells to collagen types I and III in a dose-dependent manner, but not to type IV, indicating that AAPP competes with GPVI for the binding to collagen types I and III, but not to type IV.

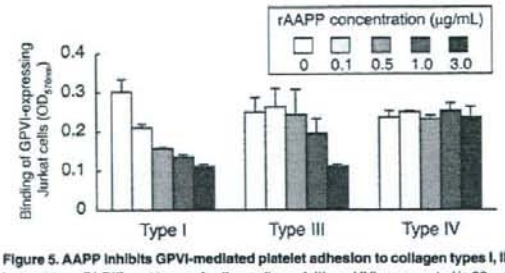

Figure 5. AAPP inhibits GPVI-mediated platelet adhesion to collagen types I, III, but not type IV. Different types of collagen (types I, III, and IV) were coated in 96-well plates. The indicated concentrations of rAAPP were added to each well and incubated for 1 hour. After washing, GPVI-expressing Jurkat cells were allowed to adhere to each well for 1 hour. After washing, adhesion cells were quantified fluorometrically. The top box indicates the concentration of rAAPP (μg/mL). Results are representative of 3 independent experiments and expressed as the mean of triplicate reading plus or minus SEM for the indicated concentrations.

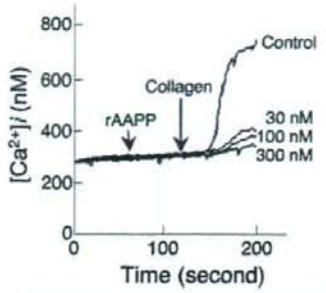

Figure 6. Effect of AAPP on $[Ca^{2+}]i$ in the early phase of collagen stimulation. Fura-2 AM-loaded platelets were incubated with 1 mM $CaCl_2$ for 5 minutes. Collagen (0.5 μg/mL) was added after a 60-second incubation with rAAPP (30, 100 or 300 nM), and the fura-2 fluorescence was determined. Tracings are representative results of a typical experiment.

AAPP inhibits the collagen-induced increase in $[Ca^{2+}]i$

Because an increase in $[Ca^{2+}]i$ is considered to play a pivotal role in platelet aggregation, we investigated the possible involvement of AAPP in the regulation of $[Ca^{2+}]i$. Addition of collagen to a human platelet suspension in the presence of 1 mM $CaCl_2$ resulted in an increase in $[Ca^{2+}]i$ (Figure 6 control). To determine the effects of AAPP on the collagen-induced increase in $[Ca^{2+}]i$, platelets were incubated with various concentrations of rAAPP for 1 minute before their activation with collagen. Even at a low concentration (30 nM), rAAPP drastically decreased the collagen-induced change in $[Ca^{2+}]i$, and 300 nM rAAPP completely abolished the change (Figure 6).

Intravenous administration of AAPP inhibits collagen-induced platelet aggregation ex vivo in rats

rAAPP also exhibited identical inhibition of collagen-induced aggregation of rat platelets in vitro (data not shown). The in vivo effects of rAAPP were tested by giving SD rats a bolus intravenous injection of rAAPP (0.1-1.0 mg/kg) and performing ex vivo aggregation studies on citrated PRP. The ED_{50} for the aggregation inhibition was 0.3 mg/kg, and rAAPP at 1.0 mg/kg prevented all detectable collagen-induced platelet aggregation (Figure 7). ADP-induced aggregation remained unaltered, even as concentrations as high as 1.0 mg/kg. There was no significant change in platelet aggregation after rTrx injection, which was used as a negative control.

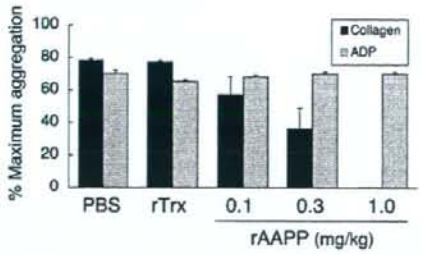

Figure 7. Inhibition of ex vivo collagen-induced aggregation of rat platelets after injection of AAPP. SD rats were administered rAAPP (0.1, 0.3, or 1.0 mg/kg) intravenously, and blood was drawn 10 minutes after the administration. Treatment with rAAPP results in inhibition of platelet aggregation in response to collagen, compared with treatment with PBS and rTrx, but has no effect on the ADP response. Results are means plus or minus SEM for 3 animals in each group.

Discussion

In the present study, we have identified and characterized an abundant saliva protein, AAPP, from the *A stephensi* mosquito. AAPP has characteristic features of acidic secreted proteins with a glycine and glutamic acid-rich region, and is specifically expressed in the distal lateral lobes of the adult female salivary glands. This expression pattern is consistent with the finding in our previous study on transgenic mosquitoes that the strong *aapp* promoter specifically drives foreign gene expression in the distal lateral lobes.[11] We have demonstrated that AAPP is unique in that it specifically blocks platelet adhesion to collagen and subsequent platelet aggregation.

Regarding the mechanism by which AAPP specifically inhibits collagen-induced platelet aggregation, AAPP directly binds to collagen I and III, and interferes with the interaction between collagen and its receptor GPVI on platelets, thereby inhibiting an increase in $[Ca^{2+}]i$, which is an important second messenger in the platelet activation cascade. The current view of collagen-induced platelet activation is that collagen initially interacts with GPVI and integrin $\alpha_2\beta_1$, and platelet activation signals are then conveyed by GPVI (reviewed in Nieswandt and Watson[36]). However, we excluded the possibility of direct interactions between AAPP and these molecules by the following pieces of evidence: (1) the 2 GPVI receptor agonists, CRP and convulxin did not compete with AAPP for platelet aggregation; (2) GPVI-expressing Jurkat cells did not bind to AAPP; and (3) the sequence motifs of the specific $\alpha_2\beta_1$ ligand, GFOGER-GPP,[37] within the collagen triple-helical region and the RGD fibrinogen receptor antagonist were not contained in the AAPP sequence. Our recent investigations have shown that, although the GE-rich region located in the N-terminal half of AAPP shows 65% similarity with the triple-helix region of the α-1 chain of human collagen IV (Figure S1B), this region is involved in the binding neither to GPVI (Figure 5E) nor collagen (S.Y. and T.S., unpublished data, July 2005). Further studies are currently in progress to identify AAPP receptor on collagen by using truncated rAAPPs.

To develop new therapeutic agents for the treatment of cardiovascular and ischemic disorders, a number of new exogenous factors have recently been identified from animal sources, and the search is still on for novel factors that interfere with platelet aggregation and blood coagulation (reviewed in Kini[38]). Although some factors effectively affect platelet function and aggregation in vitro, most of them fail to retain their biochemical and pharmacologic characteristics in vivo. To date, limited numbers of drugs have been developed or are in the process of being developed from animal sources, for example, desmoteplase (a plasminogen activator) from vampire bat saliva,[39-41] calin (a plasminogen activator) from *Hirudo medicinalis* leech saliva[42,43]; and hirudin (an anticoagulant) from *H medicinalis* leech saliva.[44,45] Our finding that intravenously administered rAAPP strongly inhibited collagen-mediated platelet aggregation ex vivo in rats may provide a potential use of AAPP for developing new drugs that maintain the flow of blood.

Malaria transmitted by anopheline mosquitoes is the worst health problem in the world, and kills 1 to 2 million people every year. Our recent studies on malaria survey have shown that approximately 90% of people living in the Solomon Islands, where malaria is hyperendemic, have high levels of antibodies against AAPP and the antibody levels are positively correlated with the antibody levels against malaria antigens (data not shown). From the

aspect of malaria epidemiology, this information may provide important insights regarding bite exposure or monitoring the inroads of anopheline mosquitoes, thereby leading to successful prediction of the emergence of malaria. In addition, it is also of great interest to address whether high levels of anti-AAPP antibodies affect mosquito biting behavior and/or malaria infection. These studies on mosquito-malaria biology are now in progress in our laboratory.

In conclusion, we have demonstrated for the first time that AAPP is a malaria vector mosquito–derived specific antagonist of receptors that mediate the adhesion of platelets to collagen. AAPP shows no similarity to any other protein in the GenBank database, indicating that it is a novel antiplatelet aggregation protein that acts via an alternative pathway. The female salivary gland–specific AAPP expression pattern and its high levels of expression suggest that AAPP may play a critical role in facilitating location of blood vessels and preventing host hemostasis during feeding. In fact, more than 50% of antiplatelet aggregation activity in the salivary glands is brought about by AAPP (S.Y. and T.S., unpublished data, June 2005). Importantly, AAPP is an attractive molecule for developing a novel antithrombosis drug. Further studies are currently underway to understand the molecular details of the AAPP-collagen interaction and evaluate the pharmacologic effectiveness in vivo.

Acknowledgments

We would like to thank C. Seki, Y. Shimada, and K. Araki for excellent assistance with the ELISAs and handling of the mosquitoes and mice. We also thank Otsuka Pharmaceutical researchers (H. Hayashi and Y. Nagamura) for help with the rat platelet aggregation study.

This work was supported by grants from the Ministry of Education, Culture, Sports and Science of Japan (16590345 and 18390130) and Otsuka Pharmaceutical.

Authorship

Contribution: S.Y., T.S., M.N., L.T., B.S., J.K., H.W., E.L., and H.M. designed and performed the research; S.Y. and T.S. interpreted and analyzed the data; and S.Y. and T.S. wrote the paper.

Conflict-of-interest disclosure: S.Y. is a grant receiver from Otsuka Pharmaceutical, and T.S. and M.N. are employees of Otsuka Pharmaceutical. All other authors declare no competing financial interests.

Correspondence: Shigeto Yoshida, Division of Medical Zoology, Department of Infection and Immunity, Jichi Medical University, 3311-1 Yakushiji, Shimotsuke, Tochigi 329-0498, Japan; e-mail: shigeto@jichi.ac.jp.

References

1. Ribeiro JM. Role of saliva in blood-feeding by arthropods. Annu Rev Entomol. 1987;32:463-478.
2. Ruggeri ZM. Platelets in atherothrombosis. Nat Med. 2002;8:1227-1234.
3. Ribeiro JM, Rossignol PA, Spielman A. Role of mosquito saliva in blood vessel location. J Exp Biol. 1984;108:1-7.
4. Ribeiro JM, Sarkis JJ, Rossignol PA, Spielman A. Salivary apyrase of *Aedes aegypti*: characterization and secretory fate. Comp Biochem Physiol B. 1984;79:81-86.
5. Francischetti IM, Valenzuela JG, Ribeiro JM. Anophelin: kinetics and mechanism of thro+mbin inhibition. Biochem. 1999;38:16678-16685.
6. Kappe SH, Kaiser K, Matuschewski K. The *Plasmodium* sporozoite journey: a rite of passage. Trends Parasitol. 2003;19:135-143.
7. Matuschewski K, Ross J, Brown SM, Kaiser K, Nussenzweig V, Kappe SH. Infectivity-associated changes in the transcriptional repertoire of the malaria parasite sporozoite stage. J Biol Chem. 2002;277:41948-41953.
8. Francischetti IM, Valenzuela JG, Pham VM, Garfield MK, Ribeiro JM. Toward a catalog for the transcripts and proteins (sialome) from the salivary gland of the malaria vector *Anopheles gambiae*. J Exp Biol. 2002;205:2429-2451.
9. Valenzuela JG, Francischetti IM, Pham VM, Garfield MK, Ribeiro JM. Exploring the salivary gland transcriptome and proteome of the *Anopheles stephensi* mosquito. Insect Biochem Mol Biol. 2003;33:717-732.
10. Calvo E, Andersen J, Francischetti IM, et al. The transcriptome of adult female *Anopheles darlingi* salivary glands. Insect Mol Biol. 2004;13:73-88.
11. Yoshida S, Watanabe H. Robust salivary gland-specific transgene expression in *Anopheles stephensi* mosquito. Insect Mol Biol. 2006;15:403-410.
12. Brummer-Korvenkontio H, Palosuo T, Francois G, Reunala T. Characterization of *Aedes communis*, Aedes aegypti and *Anopheles stephensi* mosquito saliva antigens by immunoblotting. Int Arch Allergy Immunol. 1997;112:169-174.
13. Jariyapan N, Choochote W, Jitpakdi A, et al. A glycine- and glutamate-rich protein is female salivary gland-specific and abundant in the malaria vector *Anopheles dirus* B (Diptera: Culicidae). J Med Entomol. 2006;43:867-874.
14. Winger LA, Tirawanchai N, Nicholas J, Carter HE, Smith JE, Sinden RE. Ookinete antigens of *Plasmodium berghei*. Appearance on the zygote surface of an Mr 21 kD determinant identified by transmission-blocking monoclonal antibodies. Parasite Immunol. 10:193-207, 1988.
15. Matsumoto Y, Takizawa H, Gong X, et al. Highly potent anti-human GPVI monoclonal antibodies derived from GPVI knockout mouse immunization. Thromb Res. 2007;119:319-329.
16. Coller BS, Beer JH, Scudder LE, Steinberg MH. Collagen-platelet interactions: evidence for a direct interaction of collagen with platelet GPIa/IIa and an indirect interaction with platelet GPIIb/IIIa mediated by adhesive proteins. Blood. 1989;74:182-192.
17. Yoshida S, Kobayashi T, Matsuoka H, et al. T-cell activation and cytokine production via a bispecific single-chain antibody fragment targeted to blood-stage malaria parasites. Blood. 2003;101:2300-2306.
18. Laemmli UK. Cleavage of structual proteins during the assembly of the head of the bacteriophage T4. Nature. 1970;227:680-685.
19. Yoshida S, Matsuoka H, Luo E, et al. A single-chain antibody fragment specific for the *Plasmodium berghei* ookinete protein Pbs21 confers transmission blockade in the mosquito midgut. Mol Biochem Parasitol. 1999;104:195-204.
20. Sudo T, Tachibana K, Toga K, et al. Potent effects of novel anti-platelet aggregatory cilostamide analogues on recombinant cyclic nucleotide phosphodiesterase isozyme activity. Biochem Pharmacol. 2000;59:347-356.
21. Kappes JC, Wu X, Wakefield JK. Production of trans-lentiviral vector with predictable safety. Meth Mol Med. 2003;76:449-465.
22. Nakamura T, Jamieson GA, Okuma M, Kambayashi J, Tandon NN. Platelet adhesion to native type I collagen fibrils. Role of GPVI in divalent cation-dependent and -independent adhesion and thromboxane A2 generation. J Biol Chem. 1998;273:4338-4344.
23. Sudo T, Ito H, Hayashi H, Nagamura Y, Toga K, Yamada Y. Genetic strain differences in platelet aggregation and thrombus formation of laboratory rats. Thromb Haemost. 2007;97:665-672.
24. Morol M, Jung SM, Okuma M, Shinmyozu K. A patient with platelets deficient in glycoprotein VI that lack both collagen-induced aggregation and adhesion. J Clin Invest. 1989;84:1440-1445.
25. Clemetson JM, Polgar J, Magnenat E, Wells TN, Clemetson KJ. The platelet collagen receptor glycoprotein VI is a member of the immunoglobulin superfamily closely related to FcaR and the natural killer receptors. J Biol Chem. 1999;274:29019-29024.
26. Nieswandt B, Brakebusch C, Bergmeier W, et al. Glycoprotein VI but not $\alpha_2\beta_1$ integrin is essential for platelet interaction with collagen. EMBO J. 2001;20:2120-2130.
27. Asselin J, Gibbins JM, Achison M, et al. A collagen-like peptide stimulates tyrosine phosphorylation of syk and phospholipase C g2 in platelets independent of the integrin $\alpha_2\beta_1$. Blood. 1997;89:1235-1242.
28. Francischetti IM, Saliou B, Leduc M, et al. Convulxin, a potent platelet-aggregating protein from Crotalus durissus terrificus venom, specifically binds to platelets. Toxicon. 1997;35:1217-1228.
29. Jandrot-Perrus M, Lagrue AH, Okuma M, Bon C. Adhesion and activation of human platelets induced by convulxin involve glycoprotein VI and integrin $\alpha_2\beta_1$. J Biol Chem. 1997;272:27035-27041.
30. Santoro SA, Rajpara SM, Staatz WD, Woods VL Jr. Isolation and characterization of a platelet surface collagen binding complex related to VLA-2. Biochem Biophys Res Commun. 1988;153:217-223.
31. Nieuwenhuis HK, Akkerman JW, Houdijk WP, Sixma JJ. Human blood platelets showing no response to collagen fail to express surface glycoprotein Ia. Nature. 1985;318:470-472.
32. Staatz WD, Rajpara SM, Wayner EA, Carter WG, Santoro SA. The membrane glycoprotein Ia-IIa (VLA-2) complex mediates the Mg^{2+}-dependent adhesion of platelets to collagen. J Cell Biol. 1989;108:1917-1924.

33. Zijenah LS, Morton LF, Barnes MJ. Platelet adhesion to collagen. Factors affecting Mg^{2+}-dependent and bivalent-cation-independent adhesion. Biochem J. 1990;268:481-486.
34. Jung SM, Moroi M. Platelets interact with soluble and insoluble collagens through characteristically different reactions. J Biol Chem. 1998;273:14827-14837.
35. Siljander P, Lassila R. Studies of adhesion-dependent platelet activation: distinct roles for different participating receptors can be dissociated by proteolysis of collagen. Arterioscler Thromb Vasc Biol. 1999;19:3033-3043.
36. Nieswandt B, Watson SP. Platelet-collagen interaction: is GPVI the central receptor? Blood. 2003; 102:449-461.
37. Knight CG, Morton LF, Peachey AR, Tuckwell DS, Farndale RW, Barnes MJ. The collagen-binding A-domains of integrins a_1b_1 and a_2b_1 recognize the same specific amino acid sequence, GFOGER, in native (triple-helical) collagens. J Biol Chem. 2000;275:35-40.
38. Kini RM. Platelet aggregation and exogenous factors from animal sources. Curr Drug Targets Cardiovasc Haematol Disord. 2004;4:301-325.
39. Gardell SJ, Duong LT, Diehl RE, et al. Isolation, characterization, and cDNA cloning of a vampire bat salivary plasminogen activator. J Biol Chem. 1989;264:17947-17952.
40. Furlan AJ, Eyding D, Albers GW, et al. Dose Escalation of Desmoteplase for Acute Ischemic Stroke (DEDAS): evidence of safety and efficacy 3 to 9 hours after stroke onset. Stroke. 2006;37: 1227-1231.
41. Witt W, Baldus B, Bringmann P, Cashion L, Donner P, Schleuning WD. Thrombolytic properties of *Desmodus rotundus* (vampire bat) salivary plasminogen activator in experimental pulmonary embolism in rats. Blood. 1992;79:1213-1217.
42. Deckmyn H, Stassen JM, Vreys I, Van Houtte E, Sawyer RT, Vermylen J. Calin from *Hirudo medicinalis*, an inhibitor of platelet adhesion to collagen, prevents platelet-rich thrombosis in hamsters. Blood. 1995;85:712-719.
43. Harsfalvi J, Stassen JM, Hoylaerts MF, et al. Calin from *Hirudo medicinalis*, an inhibitor of von Willebrand factor binding to collagen under static and flow conditions. Blood. 1995;85: 705-711.
44. Fareed J, Callas D, Hoppensteadt DA, Lewis BE, Bick RL, Walenga JM. Antithrombin agents as anticoagulants and antithrombotics: implications in drug development. Semin Hematol. 1999;36: 42-56.
45. Tardy B, Lecompte T, Boelhen F, et al. Predictive factors for thrombosis and major bleeding in an observational study in 181 patients with heparin-induced thrombocytopenia treated with lepirudin. Blood. 2006;108:1492-1496.

Plasmodium vivax parasites alter the balance of myeloid and plasmacytoid dendritic cells and the induction of regulatory T cells

Kulachart Jangpatarapongsa[*1,2], *Patchanee Chootong*[*1,2], *Jetsumon Sattabongkot*[3], *Kesinee Chotivanich*[4], *Jeeraphat Sirichaisinthop*[5], *Sumalee Tungpradabkul*[6], *Hajime Hisaeda*[7], *Marita Troye-Blomberg*[8], *Liwang Cui*[9] *and Rachanee Udomsangpetch*[1,2]

[1] Department of Clinical Microbiology, Faculty of Medical Technology, Mahidol University, Bangkok, Thailand
[2] Department of Pathobiology, Faculty of Science, Mahidol University, Bangkok, Thailand
[3] Department of Entomology, Armed Forces Research Institute of Medical Sciences, Bangkok, Thailand
[4] Department of Clinical Tropical Medicine, Faculty of Tropical Medicine, Mahidol University, Bangkok, Thailand
[5] Center of Malaria Research and Training, Ministry of Public Health, Saraburi, Thailand
[6] Department of Biochemistry, Faculty of Science, Mahidol University, Bangkok, Thailand
[7] Department of Parasitology, Faculty of Medical Science, Kyushu University, Fukuoka, Japan
[8] Department of Immunology, Wenner-Gren Institute, Stockholm University, Stockholm, Sweden
[9] Department of Entomology, The Pennsylvania State University, PA, USA

Immunity induced by *Plasmodium vivax* infections leads to memory T-cell recruitment and activation during subsequent infections. Here, we investigated the role of regulatory T cells (Treg) in coordination with the host immune response during *P. vivax* infection. Our results showed a significant increase in the percentage of FOXP3$^+$ Treg, IL-10-secreting Type 1 Treg (Tr1) and IL-10 levels in patients with acute *P. vivax* infection as compared with those found in either naïve or immune controls. The concurrent increase in the Treg population could also be reproduced *in vitro* using peripheral blood mononuclear cells from naïve controls stimulated with crude antigens extracted from *P. vivax*-infected red blood cells. Acute *P. vivax* infections were associated with a significant decrease in the numbers of DC, indicating a general immunosuppression during *P. vivax* infections. However, unlike *P. falciparum* infections, we found that the ratio of myeloid DC (MDC) to plasmacytoid DC (PDC) was significantly lower in acute *P. vivax* patients than that of naïve and immune controls. Moreover, the reduction in PDC may be partly responsible for the poor antibody responses during *P. vivax* infections. Taken together, these results suggest that *P. vivax* parasites interact with DC, which alters the MDC/PDC ratio that potentially leads to Treg activation and IL-10 release.

Key words: Dendritic cell · IL-10 · Malaria · *Plasmodium vivax* · Regulatory T cell

Correspondence: Professor Rachanee Udomsangpetch
e-mail: scrudmu@yahoo.com

*These authors contributed equally to this work.

Introduction

Malaria is a common tropical disease causing deaths among *Plasmodium falciparum*-infected children mainly in Sub-Saharan Africa [1]. *P. falciparum* causes malignant tertian malaria that accounts for most malaria-associated deaths, whereas *P. vivax* causes relapsing fever and the infection rarely becomes fatal. Although a better understanding of immunity is needed for the design of effective vaccines, immune regulation in the host during malaria infection is not fully understood, and few studies have been conducted in patients with *P. vivax* infections. Our recent study has shown that anti-*P. vivax* antibody levels were very low in immune individuals living in endemic area and in patients with acute *P. vivax* malaria. For the cell-mediated arm, an acute *P. vivax* infection was associated with the activation of memory T cells belonging to either a cytotoxic or helper phenotype [2]. Additionally, previous evidence [3, 4] shows that immunization with pre-erythrocytic antigens can induce IFN-γ release. This suggests that *P. vivax* can activate the immune system via the Th1 pathway. However, a possible suppressing mechanism arises from the activation of regulatory T cells (Treg) as has been shown in a murine malaria study [5].

Treg constitutively express CD25, which is the IL-2/α chain receptor [6]. Co-presentation of CD25 with forkhead box protein P3 (FOXP3) dictates the immune-suppressive role of Treg *via* the release of IL-10 and TGF-β [7]. Treg have been shown to alter the balance between myeloid dendritic cells (MDC) and plasmacytoid dendritic cells (PDC) in blood, which eventually determines the outcome of T-cell responses [8]. The increase in MDC/PDC ratio is associated with the activation of the Th1 pathway, whereas a decreased ratio is associated with the activation of the Th2 pathway [8–10]. In a murine malaria model, the parasites have been shown to evade the immune response *via* activation of Treg [11]. A recent study confirms this trend during *P. falciparum* infections where Treg activation was correlated with higher rates of parasite growth [12]. However, the role of Treg during the course of *P. vivax* infection has not been investigated. Here, we compared Treg population and IL-10 levels among acute *P. vivax* patients, immune and naïve controls. Results revealed significant association between vivax infections with increased levels of Treg and IL-10. In contrast, *P. vivax* infections led to a general reduction in DC and lowered the MDC/PDC ratio, suggesting a possible immunosuppressive role of Treg during acute *P. vivax* infections.

Results

Activation of Treg during *P. vivax* infection

The percentage of $CD4^+CD25^+$ T cells was quantified and the results are shown in Fig. 1A. Immune individuals living in endemic areas had a similar level of Treg as observed in naïve controls. However, the level was significantly elevated during acute *P. vivax* infections (mean, quartile percentages = 13.8%, 11.3–16.2) when compared with that of naïve controls (7.5%, 6.3–8.8, $P = 0.001$) and immune controls (4.3, 4.7–9.9, $P = 0.001$).

The expression of $FOXP3^+$ on $CD4^+CD25^+$ T cells was analyzed to differentiate the $FOXP3^+$ Treg [13]. The results showed that $FOXP3^+$ Treg in the acute *P. vivax* malaria patients (20.8%, 12.9–68.3) were approximately 7- and 3-fold higher than that of immune controls (2.7%, 1.9–4.6, $P < 0.001$) and naïve controls (6.3%, 2.4–10.2, $P < 0.001$), respectively. Interestingly, the level of $FOXP3^+$ Treg in the malaria immune controls was significantly lower than that in naïve controls ($P = 0.4$) (Fig. 1B).

IL-10 and the activation of Treg

It is known that Treg produce the anti-inflammatory cytokine IL-10. Results indicated that IL-10 was 4-fold higher during acute *P. vivax* infections than those measured in immune controls ($P < 0.001$) and 2-fold higher than that of naïve controls ($P = 0.005$) (Fig. 2A). The levels of IL-10 in plasma collected from immune controls were significantly lower than that seen in naïve controls ($P = 0.008$). As expected, the level of IL-10 producing Treg ($CD4^+CD25^+IL\text{-}10^+$ or type 1 Treg or "Tr1" cells) of *P. vivax* infected patients was also significantly higher than that of immune controls ($P = 0.001$) and naïve controls ($P = 0.004$) (Fig. 2B). Moreover, there was a significant association in the numbers of $FOXP3^+$ Treg and Tr1 cells in acute *P. vivax* patients ($R^2 = 0.3$, $P = 0.006$) and immune controls ($R^2 = 0.4$, $P = 0.01$). This association was not found in naïve controls (Fig. 2C).

Treg stimulation by *P. vivax* antigens

Infection with *P. vivax* resulted in an increase levels of Treg and plasma IL-10. To reproduce these phenomena *in vitro*, peripheral blood mononuclear cells from naïve controls were stimulated with *P. vivax* antigens and the number of $FOXP3^+$ Treg was determined on day 5 (Fig. 3A). The results indicated that the number of $FOXP3^+$ Treg was significantly increased when PBMC was stimulated with 50 μg/mL of *P. vivax* antigen as compared with that of normal red blood cells (NRBC) ($P = 0.01$) and that of phytohemagglutinine ($P = 0.01$). Consistent with enzyme-linked immunosorbent assay (ELISA) results, the levels of Tr1 cells measured from flow cytometric (FCM) analysis was found to increase after stimulation with 50 μg/mL of *P. vivax* antigen as compared with that of NRBC ($P = 0.048$) (Fig. 3B). Moreover, in reverse transcriptase-polymerase chain reaction (PCR) we also detected the expression of IL-10 in naïve PBMC after 5 days of stimulation with *P. vivax* antigens (data not shown).

Blood DC during acute *P. vivax* infection

Circulating DC defined as $HLA\text{-}DR^+$MDC and $HLA\text{-}DR^+$PDC were determined in acute *P. vivax* patients and naïve controls

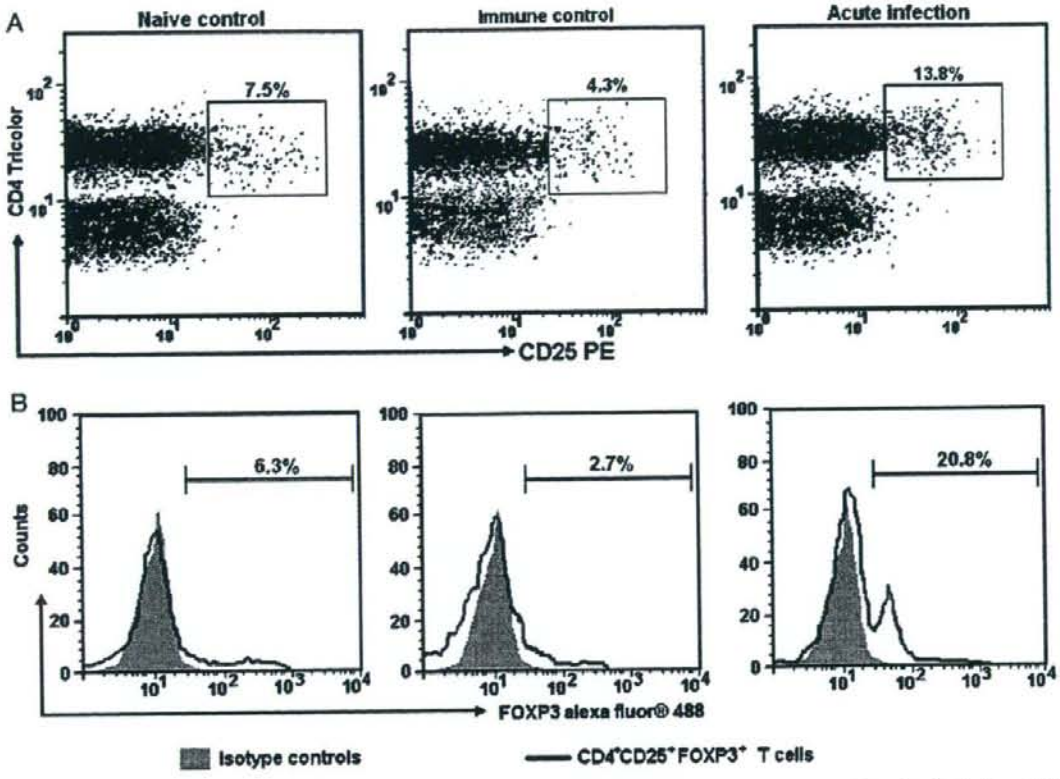

Figure 1. Increased numbers of FOXP3$^+$ Treg in patients with acute *P. vivax* infections. FCM analyses of cryopreserved PBMC stained with anti-CD4 Tricolor, anti-CD25 PE, and anti-FOXP3 Alexa Fluor® 488 from the indicated groups and lymphocyte populations were gated. (A) CD4$^+$CD25$^+$ T cells in the lymphocyte population are indicated by the boxed areas. (B) Histograms of FOXP3 expression in the CD4$^+$CD25$^+$ T cells. The percentages of CD4$^+$CD25$^+$ (A) and CD4$^+$CD25$^+$FOXP3$^+$ (B) cells are shown. All figures show one representative sample out of seventeen.

(Fig. 4A–C). The results showed that the absolute numbers of both MDC and PDC were significantly reduced in *P. vivax* patients than those of naïve controls ($P = 0.09$ and 0.03, respectively) (Fig. 4D). Consequently, the MDC/PDC ratio was significantly different between naïve controls and acute *P. vivax* patients ($P = 0.01$) (Fig. 4E).

During infection, *P. vivax* parasites may activate Treg via *P. vivax*-primed MDC or PDC of the host. Therefore, the association between MDC or PDC with Treg was analyzed. However, there was no association between PDC or MDC with FOXP3$^+$ Treg or Tr1 cells (data not shown).

Discussion

Infections by pathogens can lead to either the Th1 or Th2 response. Th1 response often leads to the resolution of malaria infection and therefore is favored in vaccine design [14]. IFN-γ produced by CD8 T cells and/or NK cells inhibits parasite development, thereby contributing to the protection against pre-erythrocytic stages of both *P. falciparum* and *P. vivax* [15]. However, there are studies showing the induction of IL-10 in malaria patients, suggesting that Th2 pathway may also be involved in malaria immunity [16]. Quite different from the findings in *P. falciparum*, we found that *P. vivax* infections rarely resulted in significant production of parasite-specific antibodies, but that acute *P. vivax* infections induced Treg activation. This result is consistent with two recent findings in both *P. yoelii* and *P. falciparum*, suggesting that parasites may use a similar mechanism of immune evasion [11, 12]. Although the interactions among malaria-specific T cells, B cells and Treg remain poorly characterized, our result suggested that the increased frequency of Treg during acute *P. vivax* infection may lead to suppression of both cell- and antibody-mediated immunities, which may benefit parasite survival in hosts. There are evidence indicating that Treg can suppress T-cell responses through the production of IL-10 and TGF-β [17, 18], whereas they may suppress B-cell maturation and differentiation directly [19, 20] or indirectly through the down-regulation of IL-2 or IL-4 production in responder lymphocytes. This may account for low parasite-specific antibody levels seen in *P. vivax* patients [2].

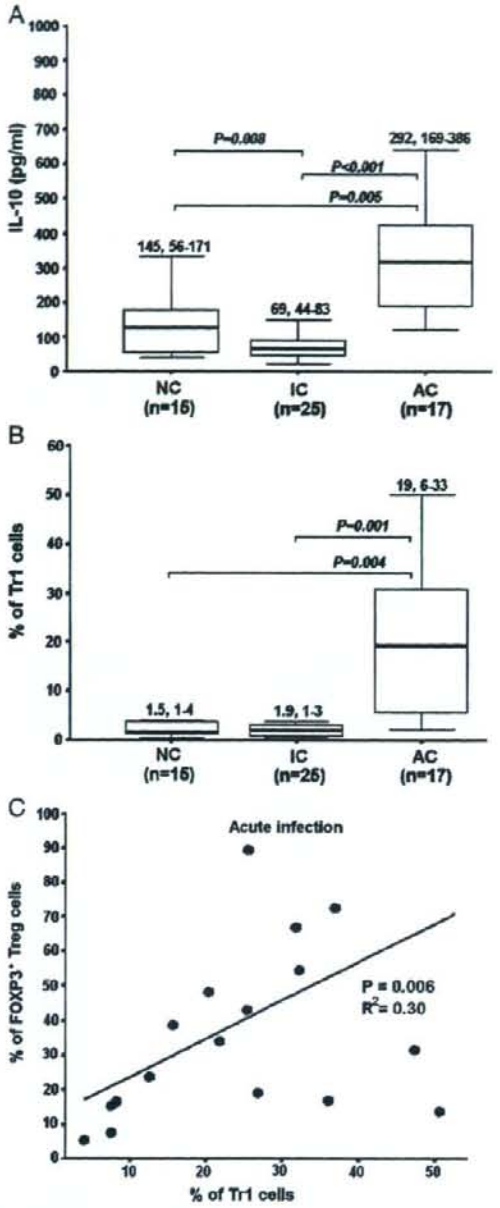

Figure 2. Comparison of the levels of plasma IL-10 (A) and Tr1 cells (B) between naïve controls (NC), immune controls (IC), and patients acutely infected with *P. vivax* (AC). The correlation between Tr1 cells and FOXP3$^+$ Treg in lymphocytes from patients acutely infected with *P. vivax* (C). Data are shown as mean (thick horizontal line), inter-quartile range (box plot), maximum and minimum (upper–lower lines) (A and B). The numbers represent mean, inter-quartile range. (Data were log transformed and independent sample t test was used to calculate *P* value).

In this study, patients with acute *P. vivax* infection were observed to exhibit higher plasma levels of IL-10 than those of naïve and immune controls. Similar findings have been reported in both *P. vivax* and *P. falciparum* infections [21–24]. Even though there is evidence that CD8 Treg produce IL-10 to suppress T-cell responses [25], our result showed a significant correlation between elevated levels of Tr1 and FOXP3$^+$ Treg, a result further corroborating our earlier finding of increased levels of total CD4$^+$ T cells during acute *P. vivax* infections [2]. In parallel, we also found a concurrent increased levels of Treg and expression of IL-10 when PBMC from naive controls were stimulated with *P. vivax* antigens *in vitro*. This result is also consistent with findings that the number of Treg is increased in cord blood mononuclear cells of placental *P. falciparum* infections and IL-10 elevation after stimulation with *P. falciparum* antigens [26]. Altogether, these results suggest that Treg may be a direct source of IL-10 production and/or enhance the IL-10 production by DC [27]. Recent report showing that the stimulated FOXP3$^+$ Treg produce many cytokines including IL-10 resulting in activation of monocytes/macrophages can support the former hypothesis [28]. Our finding showed significant association between different Treg populations during acute *P. vivax* infection, despite the fact that some acutely infected cases (23%) appeared to have elevated proportion of Tr1 cells with comparatively low levels of FOXP3$^+$ Treg. Previous studies have demonstrated that Tr1 cells generated *in vitro* do not express FOXP3$^+$, but it was found to maintain the suppressor function [29, 30]. This suggests that FOXP3 expression is not a prerequisite for the suppressive function of Tr1 cells. On the other hand, Tr1 cells specific for desmoglein3, the dominant autoantigen in pemphigus vulgaris, are shown to constitutively express FOXP3 [31]. Therefore, the association of Tr1 cells with FOXP3$^+$ Treg remains controversial and needs further investigation [32].

Among the three groups of volunteers, the lowest levels of IL-10 and Tr1 cells were observed in the immune controls. This suggests that the activation of Treg is transient during *P. vivax* infections and that subsequent decline in Treg after parasite clearance could be due to higher levels of memory T cells that were maintained after the infection [2]. Our study did not find a correlation of CD4$^+$CD25$^+$ and FOXP3 levels. This result is in line with a recent study showing no correlation between CD25$^+$ cells and FOXP3 level in human CD4$^+$ cells [33].

The immunoregulatory effect of malaria infections is related with the down-regulation of antigen presenting DC. Consistent with earlier studies documenting the immunosuppressive effect of malaria parasites on the maturation and differentiation of DC [34, 35], we found significantly lower levels of DC (both PDC and MDC) in acute *P. vivax* patients. This finding coincides with the recent study showing the decreasing numbers of MDC and PDC among children with severe *P. falciparum* infection [36]. Another reason could be the reallocation of cells away from the peripheral blood, *e.g.* to the spleen. The evidence of lymphopenia in both *P. falciparum* and *P. vivax* infection supports such an explanation [37–39]. The levels of MDC and PDC in the peripheral blood are recovered during post-treatment [36].

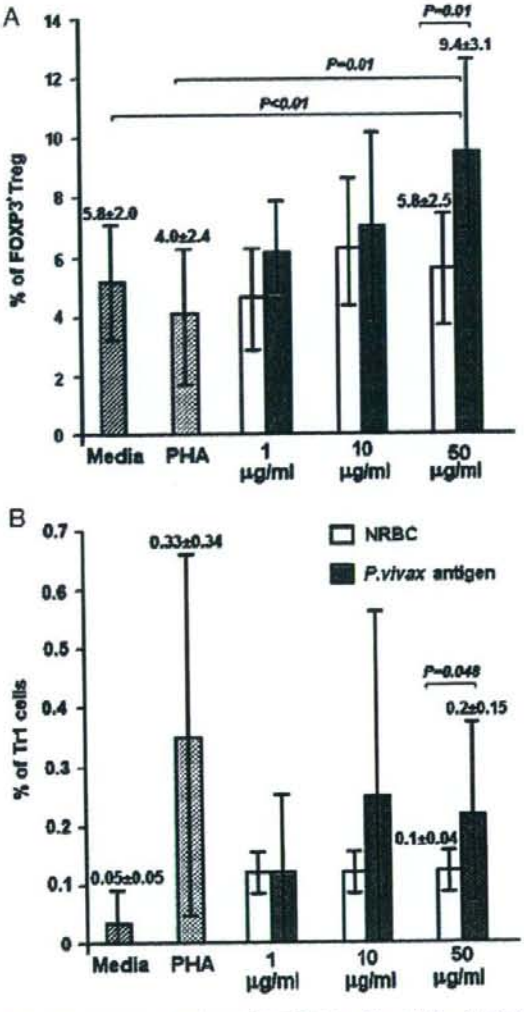

Figure 3. Increased numbers of FOXP3$^+$ Treg (A) and Tr1 cells (B) in lymphocytes after stimulation with P. vivax antigens. PBMC from naïve controls cultured with NRBC or PV schizont lysate at the indicated concentrations were analyzed for FCM analysis. Data represent mean percentage ± SD of five experiments. Data were log transformed and independent sample t test was used to calculate P value.

It has been shown that the depletion of PDC abrogated the secretion of specific polyclonal IgG in response to influenza virus [40]. Therefore, the reduction in PDC level during *P. vivax* infection may account for the low level of *P. vivax*-specific antibodies in vivax patients [2]. This suggests that PDC are critical for the generation of plasma cells and antibody responses during parasite/pathogen infections. However, unlike that of *P. falciparum*-infected patients [36], the percentage of PDC was higher than that of MDC during acute *P. vivax* infections, resulting in a lower MDC/PDC ratio. This may suggest that *P. vivax* parasites suppress host immune response through elevated levels of PDC and Treg. Two pieces of evidence show that the stimulation of PDC induces naïve CD4 and CD8 T-cell differentiation into Th2 cells and IL-10 producing CD8 T-cells [8, 41].

Taken together, we found that acute *P. vivax* infections were associated with higher levels of Treg and IL-10, but lower levels of DC in the blood. This suggests that Treg are activated by parasites during acute infections, which then play an immunosuppressive role of host cell- and antibody-mediated immunities, resulting in retarded parasite clearance. While the overall levels of DC were reduced, the balance between the two cell types (MDC and PDC) was altered. In addition, our previous study also revealed an increase in the levels of γδ T cells during acute *P. vivax* infection. Therefore, the interactions among different DC, T cell phenotypes and *P. vivax* antigens await further investigations.

Materials and methods

Study population

Blood samples were collected from 17 patients with acute *P. vivax* infections at two malaria clinics in Mae Sot and Mae Kasa, Tak province, Thailand. Diagnosis of *P. vivax* malaria infection was based on the examination of Giemsa-stained thick blood films. PCR with four human malaria (*P. falciparum*, *P. vivax*, *P. malariae*, and *P. ovale*) species-specific primers was performed on DNA isolated from blood samples to verify malaria infections. Only single *P. vivax* infection was recruited in the experiments. Blood samples were collected from 25 additional people residing in the same *P. vivax*-endemic area. The subjects defined as "immune controls" have had recent malaria infections and had anti-*P. vivax* antibodies determined by ELISA. These immune controls did not have *P. vivax* infections at the time of blood collection as determined by both microscopic and PCR analyses. Fifteen healthy adults living in Bangkok without previous malaria exposure or antibodies to malaria parasites were recruited to serve as "naïve controls". The clinical characteristics of the subjects are listed in Table 1. This study was approved by the Committee on Human Rights Related to Human Experimentation, Mahidol University, and the Ministry of Health, Thailand. Informed consent was obtained from each individual before the blood sample was taken.

Preparation and cryopreservation of PBMC

Venous blood from *P. vivax* patients, immune controls, and naïve controls was collected in heparinized tubes and PBMC were separated by gradient centrifugation using Lymphoprep™ (AXIS-Shied PoC AS, Oslo, Norway) according to the manufacturer's

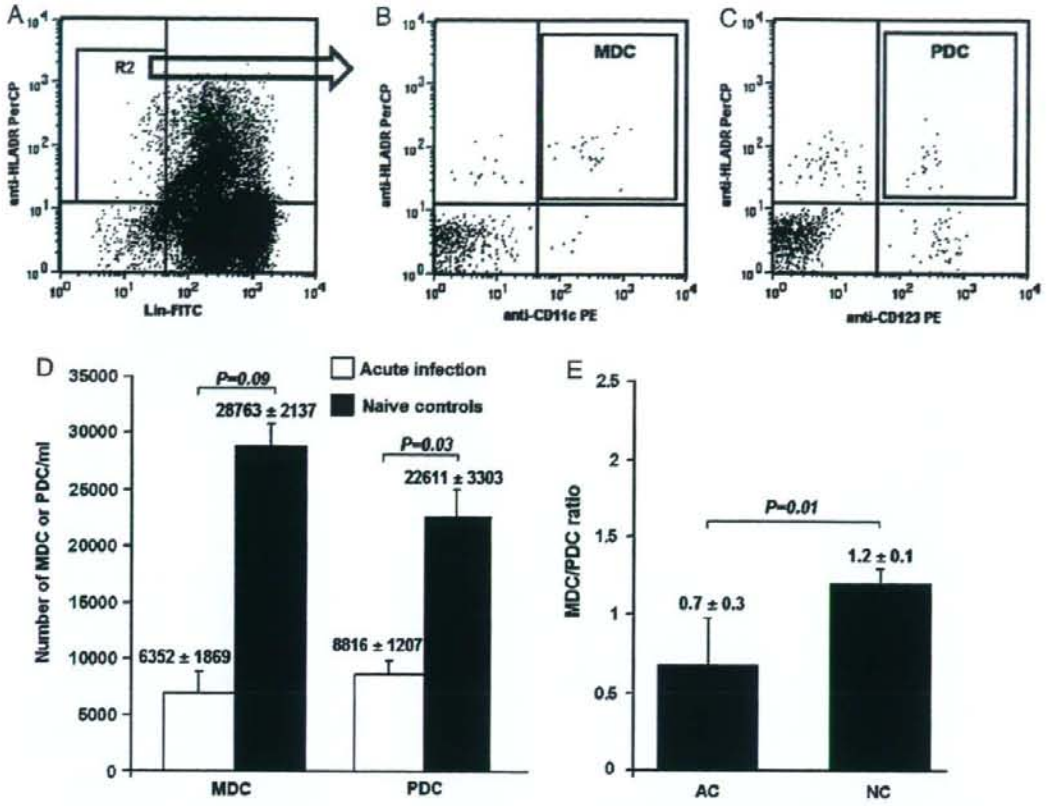

Figure 4. (A–C) FCM analyses of whole blood stained with anti-HLA-DR PerCP and Lin FITC, anti-CD11c RPE (for MDC), or anti-CD123 RPE (for PDC) R2 shows the population of HLA-DR$^+$Lin$^-$. (D) Number of MDC and PDC. (E) MDC/PDC ratio in the peripheral blood of patients acutely infected with *P. vivax* (AC) and naïve controls (NC). Numbers represent mean ± SD. (number of samples: acute infections = 17 and naïve controls = 15) Sample t test was used to calculate P value.

Table 1. Information and clinical data of *P. vivax* patients, immune and naïve controls[a)]

	No. of cases	Age (years)	Sex		Hematocrit (%)	Temperature (°C)	Parasitemia (%)
			M	F			
AC	17	38±11 (15–52)	7	10	43±7 (35–63)	37.5±1.3 (35–40)	0.4±0.3 (0.03–1.2)
IC	25	38±13 (18–77)	16	9	46±3 (43–48)	36.8±0.4 (36–37)	0
NC	15	29±7 (22–43)	8	7	42±4 (37–45)	37.0±0.5	0

[a)] Mean ± standard deviation (range). AC, acute *P. vivax* infection; IC, immune controls; NC, naïve controls.

recommendations. The PBMC pellet was resuspended at a concentration of 10^6 cells/mL in RPMI-1640 supplemented with 10% heat-inactivated fetal bovine serum (Invitrogen, Carlsbad, USA). The viability of PBMC, normally above 98%, was determined by tryphan blue exclusion. PBMC in 10% dimethyl sulfoxide were cryopreserved in liquid nitrogen until analysis.

Parasite cultures and antigen preparations

Crude *P. vivax* antigens were obtained from *P. vivax*-infected red blood cells. Briefly, *P. vivax*-infected blood was depleted of white blood cells by filtering through a sterile column of CF11 cellulose (Whatman, Maidstone, UK) and the RBC were washed

with RPMI-1640 by centrifugation at 1190g for 5 min. The parasites were cultured in an atmosphere of 5% CO_2, 5% O_2, and 90% N_2 for 24–30 h at 5% hematocrit in McCoy's 5A medium (Invitrogen) supplemented with 25% human AB serum until they matured to the schizont stage (≥six nuclei). These mature parasites were enriched by centrifugation on 60% Percoll (Pharmacia, Uppsala, Sweden) at 1190g for 10 min. The enriched infected red blood cell pellets were sonicated for 40 s at 150 watts and the protein concentration was determined by the Bradford assay (Bio-Rad, Hercules, USA). The vials were then aliquoted and stored at −70°C until use. Uninfected RBC were processed similarly and stored at −70°C to be used as a negative control.

In vitro stimulation of PBMC

PBMC from five healthy donors were used for *in vitro* stimulation. PBMC (2×10^5 cells/well) in RPMI-1640 supplemented with 25 mM HEPES, 1.8 mg/mL D-glucose, 2 mM glutamine, 40 mg/mL of gentamicin, and 10% heat-inactivated fetal bovine serum were cultured for 5 days at 37°C in a humidified chamber with 5% CO_2, 5% O_2, and 90% N_2 in the presence of *P. vivax* antigens at a concentration of 1, 10, or 50 μg/mL. Medium alone, equivalent concentration of RBC extracts or 2 μg/mL of phytohemagglutinine were used as negative and positive controls, respectively. All the experiments were performed in duplicates. After 5 days of activation, the cells were harvested and stained for Treg marker, CD25 and FOXP3 or IL-10.

Intracellular staining and FCM analysis

For the three-color FCM analysis, PBMC (10^5 cells/vial) were stained with a combination of fluorochrome-conjugated monoclonal antibodies (mAbs): RPE-Cy5-labeled anti-CD4 (Caltag, Burlingame, USA) and RPE-labeled anti-CD25 (Immunotech, Marseille, France) for 30 min at 4°C and washed with phosphate-buffered saline (PBS). After staining, the cell pellets were fixed with a fixative solution and washed with a permeabilizing solution according to the manufacturer's recommendations (BioLegend, San Diego, USA). After incubation in the permeabilizing buffer for 20 min at room temperature, the cells were incubated with Alexa fluor® 488-labeled anti-FOXP3 (BioLegend) or FITC-labeled anti-IL-10 for 30 min and then washed with PBS. Cells were fixed with the fixative solution for data acquisition and analysis on FACSCalibur using the CELLQUEST software (Becton Dickinson, San Jose, USA).

Phenotyping of circulating blood DC

Two hundred microliters of whole blood from *P. vivax*-infected patients were stained with an antibody mixture containing lineage-specific mAbs to CD3, CD14, CD19, CD20, CD56, and CD66b conjugated with FITC (lin-FITC) (Caltag), antibodies to CD11c (Serotec, Oxford, UK) and CD123 conjugated with RPE (BioLegend), and antibodies to HLA-DR conjugated with PerCP (Becton Dickinson). Stained cells were treated with RBC lysis solution. At least 2×10^5 cells were analyzed in a FACSCalibur flow cytometer (Becton Dickinson). HLA-DR$^+$CD123$^+$lin$^-$ cells were defined as PDC and HLA-DR$^+$CD11c$^+$lin$^-$ as MDC. The absolute number of circulating MDC and PDC was obtained by multiplying the percentage of MDC or PDC by the number of leukocytes per milliliter of blood.

Determination of IL-10 by ELISA

Polystyrene immunoplates (Corning, Corning, USA) were coated with 25 μL of 1 g/mL of anti-human IL-10 mAb (Mabtech, Nacka, Sweden) diluted in PBS (pH 7.4) and incubated overnight at 4°C. Each well was blocked with 50 μL of 0.1% bovine serum albumin for 90 min at room temperature. After five washings with PBS, 25 μL of plasma (1:2 dilution) or PBS control were added into duplicate wells and incubated overnight at 4°C. The plates were then washed for five times with PBS, after which 25 μL of anti-human IL-10 conjugated with biotin (dilution 1:2000) were added and incubated for 90 min at 37°C, followed by the addition of 25 μL of streptavidin-alp-PQ (dilution 1:2000) (Mabtech) at 37°C for 90 min. After five final washings, 25 μL of *p*-nitro phenylphosphate (Sigma, Saint Louis, USA) were added and incubated for 30–60 min in the dark at room temperature. Enzyme activity was measured by an automated microplate reader, V-Max (Molecular Device, Sunnyvale, USA) at 405 nm.

Determination of IL-10 gene expression by reverse transcriptase-PCR

RNA was extracted from six samples after *in vitro* stimulation using Trizol® solution (Invitrogen) according to the manufacturer's recommendation. Total RNA was reverse transcribed to cDNA; primers of the IL-10 gene and amplification conditions were as described previously [42]. The expression of *IL-10* gene (138 bp) was determined in 1.5% agarose gels containing ethidium bromide. Primers of β-*actin* were designed as described previously [43] and used as a control (790 bp).

Data analysis

All data were analyzed using the SPSS program (Version 10.0, Chicago, USA). The percentages of CD4$^+$CD25$^+$, FOXP3$^+$ Treg, Tr1 phenotypes, plasma IL-10 levels, and number of MDC and PDC both from volunteers and *in vitro* stimulation were log transformed to produce normal distributions. Parametric analysis was performed using transformed data as follows: the mean percentage differences for Treg phenotypes, IL-10 levels, and number of MDC and PDC between the groups (*i.e.* naïve controls

vs. immune controls, naïve controls *vs.* acute infection, and immune controls *vs.* acute infection) were analyzed using the independent samples *t* test. The Spearman approach was used to evaluate the correlation of Tr1 with FOXP3$^+$ Treg and the correlation of MDC or PDC levels with Treg. The results were considered statistically significant ($P<0.05$) at the 95% confidence interval.

Acknowledgements: We thank all the staff at the Mae Sot and Mae Kasa Malaria Clinics, the Department of Entomology, AFRIMS, Bangkok, and the Malaria Training Center, Saraburi, Thailand, for collection of the samples. We also thank M. Hagstedt, and W. Jangiam for technical support. KJ was a research fellow supported by the Fogarty International Center (FIC), National Institutes of Health (NIH). This work was partly supported by The Thailand Research Fund to RU, by The Commission on Higher Education to KJ (CHE-RES-PD), by BioMalPar to MT and by a grant (D43-TW006571) to LC from FIC, NIH.

Conflict of interest: The authors declare no financial or commercial conflict of interest.

References

1 **Sachs, J. and Malaney, P.**, The economic and social burden of malaria. *Nature* 2002. **415**: 680–685.

2 **Jangpatarapongsa, K., Sirichaisinthop, J., Sattabongkot, J., Cui, L., Montgomery, S. M., Looareesuwan, S., Troye-Blomberg, M. and Udomsangpetch, R.**, Memory T cells protect against *Plasmodium vivax* infection. *Microbes Infect.* 2006. **8**: 680–686.

3 **Herrera, S., Bonelo, A., Perlaza, B. L., Fernandez, O. L., Victoria, L., Lenis, A. M., Soto, L. et al.**, Safety and elicitation of humoral and cellular responses in colombian malaria-naive volunteers by a *Plasmodium vivax* circumsporozoite protein-derived synthetic vaccine. *Am. J. Trop. Med. Hyg.* 2005. **73**: 3–9.

4 **Herrera, S., Bonelo, A., Perlaza, B. L., Valencia, A. Z., Cifuentes, C., Hurtado, S., Quintero, G. et al.**, Use of long synthetic peptides to study the antigenicity and immunogenicity of the *Plasmodium vivax* circumsporozoite protein. *Int. J. Parasitol.* 2004. **34**: 1535–1546.

5 **Hisaeda, H., Yasutomo, K. and Himeno, K.**, Malaria: immune evasion by parasites. *Int. J. Biochem. Cell Biol.* 2005. **37**: 700–706.

6 **Shevach, E. M.**, $CD4^+CD25^+$ suppressor T cells: more questions than answers. *Nat. Rev. Immunol.* 2002. **2**: 389–400.

7 **Wan, Y. Y. and Flavell, R. A.**, The roles for cytokines in the generation and maintenance of regulatory T cells. *Immunol. Rev.* 2006. **212**: 114–130.

8 **Rissoan, M. C., Soumelis, V., Kadowaki, N., Grouard, G., Briere, F., de Waal Malefyt, R. and Liu, Y. J.**, Reciprocal control of T helper cell and dendritic cell differentiation. *Science* 1999. **283**: 1183–1186.

9 **Kuwana, M.**, Induction of anergic and regulatory T cells by plasmacytoid dendritic cells and other dendritic cell subsets. *Hum. Immunol.* 2002. **63**: 1156–1163.

10 **Liu, Y. J.**, Dendritic cell subsets and lineages, and their functions in innate and adaptive immunity. *Cell* 2001. **106**: 259–262.

11 **Hisaeda, H., Maekawa, Y., Iwakawa, D., Okada, H., Himeno, K., Kishihara, K., Tsukumo, S. and Yasutomo, K.**, Escape of malaria parasites from host immunity requires $CD4^+CD25^+$ regulatory T cells. *Nat. Med.* 2004. **10**: 29–30.

12 **Walther, M., Tongren, J. E., Andrews, L., Korbel, D., King, E., Fletcher, H., Andersen, R. F. et al.**, Upregulation of TGF-b, Foxp3, and $CD4^+CD25^+$ regulatory T cells correlates with more rapid parasite growth in human malaria infection. *Immunity* 2005. **23**: 287–296.

13 **Shevach, E. M.**, From vanilla to 28 flavors: multiple varieties of T regulatory cells. *Immunity* 2006. **25**: 195–201.

14 **Perlmann, P. and Troye-Blomberg, M.**, *Malaria Immunology*, 2nd Edn., Karger, Basel 2002.

15 **Herrera, S., Corradin, G. and Arevalo-Herrera, M.**, An update on the search for a *Plasmodium vivax* vaccine. *Trends Parasitol.* 2007. **23**: 122–128.

16 **Kurtis, J. D., Lanar, D. E., Opollo, M. and Duffy, P. E.**, Interleukin-10 responses to liver-stage antigen 1 predict human resistance to *Plasmodium falciparum*. *Infect. Immun.* 1999. **67**: 3424–3429.

17 **Groux, H., Bigler, M., de Vries, J. E. and Roncarolo, M. G.**, Interleukin-10 induces a long-term antigen-specific anergic state in human $CD4^+$ T cells. *J. Exp. Med.* 1996. **184**: 19–29.

18 **Groux, H., O'Garra, A., Bigler, M., Rouleau, M., Antonenko, S., de Vries, J. E. and Roncarolo, M. G.**, A $CD4^+$ T-cell subset inhibits antigen-specific T-cell responses and prevents colitis. *Nature* 1997. **389**: 737–742.

19 **Lim, H. W., Hillsamer, P., Banham, A. H. and Kim, C. H.**, Cutting edge: direct suppression of B cells by $CD4^+CD25^+$ regulatory T cells. *J. Immunol.* 2005. **175**: 4180–4183.

20 **Wu, K., Bi, Y., Sun, K. and Wang, C.**, IL-10-producing type 1 regulatory T cells and allergy. *Cell. Mol. Immunol.* 2007. **4**: 269–275.

21 **Zeyrek, F. Y., Kurcer, M. A., Zeyrek, D. and Simsek, Z.**, Parasite density and serum cytokine levels in *Plasmodium vivax* malaria in Turkey. *Parasite Immunol.* 2006. **28**: 201–207.

22 **Yeom, J. S., Park, S. H., Ryu, S. H., Park, H. K., Woo, S. Y., Ha, E. H., Lee, B. E. et al.**, Serum cytokine profiles in patients with *Plasmodium vivax* malaria: a comparison between those who presented with and without hepatic dysfunction. *Trans. R. Soc. Trop. Med. Hyg.* 2003. **97**: 687–691.

23 **Prakash, D., Fesel, C., Jain, R., Cazenave, P. A., Mishra, G. C. and Pied, S.**, Clusters of cytokines determine malaria severity in *Plasmodium falciparum*-infected patients from endemic areas of Central India. *J. Infect. Dis.* 2006. **194**: 198–207.

24 **Wroczynska, A., Nahorski, W., Bakowska, A. and Pietkiewicz, H.**, Cytokines and clinical manifestations of malaria in adults with severe and uncomplicated disease. *Int. Marit. Health* 2005. **56**: 103–114.

25 **Gillet, M. and Liu, Y. J.**, Generation of human CD8 T regulatory cells by CD40 ligand-activated plasmacytoid dendritic cells. *J. Exp. Med.* 2002. **195**: 695–704.

26 **Brustoski, K., Moller, U., Kramer, M., Hartgers, F. C., Kremsner, P. G., Krzych, U. and Luty, A. J.**, Reduced cord blood immune effector-cell responsiveness mediated by $CD4^+$ cells induced in utero as a consequence of placental *Plasmodium falciparum* infection. *J. Infect. Dis.* 2006. **193**: 146–154.

27 **Veldhoen, M., Moncrieffe, H., Hocking, R. J., Atkins, C. J. and Stockinger, B.**, Modulation of dendritic cell function by naive and regulatory $CD4^+$ T cells. *J. Immunol.* 2006. **176**: 6202–6210.

28 **Tiemessen, M. M., Jagger, A. L., Evans, H. G., van Herwijnen, M. J., John, S. and Taams, L. S.**, $CD4^+CD25^+Foxp3^+$ regulatory T cells induce alternative

activation of human monocytes/macrophages. *Proc. Natl. Acad. Sci. USA* 2007. **104**: 19446–19451.

29 **Levings, M. K., Gregori, S., Tresoldi, E., Cazzaniga, S., Bonini, C. and Roncarolo, M. G.**, Differentiation of Tr1 cells by immature dendritic cells requires IL-10 but not CD25$^+$CD4$^+$Tr cells. *Blood* 2005. **105**: 1162–1169.

30 **Vieira, P. L., Christensen, J. R., Minaee, S., O'Neill, E. J., Barrat, F. J., Boonstra, A., Barthlott, T. et al.**, IL-10-secreting regulatory T cells do not express Foxp3 but have comparable regulatory function to naturally occurring CD4$^+$CD25$^+$ regulatory T cells. *J. Immunol.* 2004. **172**: 5986–5993.

31 **Veldman, C., Pahl, A., Beissert, S., Hansen, W., Buer, J., Dieckmann, D., Schuler, G. and Hertl, M.**, Inhibition of the transcription factor Foxp3 converts desmoglein 3-specific type 1 regulatory T cells into Th2-like cells. *J. Immunol.* 2006. **176**: 3215–3222.

32 **Sakaguchi, S.**, Regulatory T cells in the past and for the future. *Eur. J. Immunol.* 2008. **38**: 901–937.

33 **Liu, W., Putnam, A. L., Xu-Yu, Z., Szot, G. L., Lee, M. R., Zhu, S., Gottlieb, P. A. et al.**, CD127 expression inversely correlates with FoxP3 and suppressive function of human CD4$^+$T reg cells. *J. Exp. Med.* 2006. **203**: 1701–1711.

34 **Skorokhod, O. A., Alessio, M., Mordmuller, B., Arese, P. and Schwarzer, E.**, Hemozoin (malarial pigment) inhibits differentiation and maturation of human monocyte-derived dendritic cells: a peroxisome proliferator-activated receptor-gamma-mediated effect. *J. Immunol.* 2004. **173**: 4066–4074.

35 **Urban, B. C., Ferguson, D. J., Pain, A., Willcox, N., Plebanski, M., Austyn, J. M. and Roberts, D. J.**, *Plasmodium falciparum*-infected erythrocytes modulate the maturation of dendritic cells. *Nature* 1999. **400**: 73–77.

36 **Urban, B. C., Cordery, D., Shafi, M. J., Bull, P. C., Newbold, C. I., Williams, T. N. and Marsh, K.**, The frequency of BDCA3-positive dendritic cells is increased in the peripheral circulation of Kenyan children with severe malaria. *Infect. Immun.* 2006. **74**: 6700–6706.

37 **Hviid, L. and Kemp, K.**, What is the cause of lymphopenia in malaria? *Infect. Immun.* 2000. **68**: 6087–6089.

38 **Kassa, D., Petros, B., Mesele, T., Hailu, E. and Wolday, D.**, Characterization of peripheral blood lymphocyte subsets in patients with acute *Plasmodium falciparum* and *P. vivax* malaria infections at Wonji Sugar Estate, Ethiopia. *Clin. Vaccine Immunol.* 2006. **13**: 376–379.

39 **Richards, M. W., Behrens, R. H. and Doherty, J. F.**, Short report: hematologic changes in acute, imported *Plasmodium falciparum* malaria. *Am. J. Trop. Med. Hyg.* 1998. **59**: 859.

40 **Jego, G., Palucka, A. K., Blanck, J. P., Chalouni, C., Pascual, V. and Banchereau, J.**, Plasmacytoid dendritic cells induce plasma cell differentiation through type I interferon and interleukin 6. *Immunity* 2003. **19**: 225–234.

41 **Gilliet, M. and Liu, Y. J.**, Human plasmacytoid-derived dendritic cells and the induction of T-regulatory cells. *Hum. Immunol.* 2002. **63**: 1149–1155.

42 **Giulietti, A., Overbergh, L., Valckx, D., Decallonne, B., Bouillon, R. and Mathieu, C.**, An overview of real-time quantitative PCR: applications to quantify cytokine gene expression. *Methods* 2001. **25**: 386–401.

43 **Kokkinopoulos, I., Jordan, W. J. and Ritter, M. A.**, Toll-like receptor mRNA expression patterns in human dendritic cells and monocytes. *Mol. Immunol.* 2005. **42**: 957–968.

Abbreviations: **FCM:** flow cytometric · **FOXP3:** forkhead box protein P3 · **MDC:** myeloid DC · **NRBC:** normal red blood cell · **PDC:** plasmacytoid DC · **Tr1:** IL-10-secreting Type I Treg

Full correspondence: Professor Rachanee Udomsangpetch, Department of Pathobiology, Faculty of Science, Mahidol University, Rama VI Road, Bangkok 10400, Thailand
Fax: +662-354-7158
e-mail: scrudmu@yahoo.com

Additional correspondence: Dr. Kulachart Jangpatarapongsa, Department of Clinical Microbiology, Faculty of Medical Technology, Mahidol University, Bangkoknoi, Bangkok 10700, Thailand
Fax: +662-441-4380
e-mail: oadworld@yahoo.com

Received: 22/1/2008
Revised: 18/7/2008
Accepted: 18/7/2008

Malaria-Specific and Nonspecific Activation of CD8$^+$ T Cells during Blood Stage of *Plasmodium berghei* Infection[1]

Mana Miyakoda,* Daisuke Kimura,* Masao Yuda,‡ Yasuo Chinzei,‡ Yoshisada Shibata,† Kiri Honma,* and Katsuyuki Yui[2]*

Cerebral malaria is one of the severe complications of *Plasmodium falciparum* infection. Studies using a rodent model of *Plasmodium berghei* ANKA infection established that CD8$^+$ T cells are involved in the pathogenesis of cerebral malaria. However, it is unclear whether and how *Plasmodium*-specific CD8$^+$ T cells can be activated during the erythrocyte stage of malaria infection. We generated recombinant *Plasmodium berghei* ANKA expressing OVA (OVA-PbA) to investigate the parasite-specific T cell responses during malaria infection. Using this model system, we demonstrate two types of CD8$^+$ T cell activations during the infection with malaria parasite. Ag (OVA)-specific CD8$^+$ T cells were activated by TAP-dependent cross-presentation during infection with OVA-PbA leading to their expression of an activation phenotype and granzyme B and the development to functional CTL. These highly activated CD8$^+$ T cells were preferentially sequestered in the brain, although it was unclear whether these cells were involved in the pathogenesis of cerebral malaria. Activation of OVA-specific CD8$^+$ T cells in RAG2 knockout TCR-transgenic mice during infection with OVA-PbA did not have a protective role but rather was pathogenic to the host as shown by their higher parasitemia and earlier death when compared with RAG2 knockout mice. The OVA-specific CD8$^+$ T cells, however, were also activated during infection with wild-type parasites in an Ag-nonspecific manner, although the levels of activation were much lower. This nonspecific activation occurred in a TAP-independent manner, appeared to require NK cells, and was not by itself pathogenic to the host. ***The Journal of Immunology*****, 2008, 181: 1420–1428.**

Malaria remains one of the crucial threats to public health in much of the world. It has been well accepted that Ab and CD4$^+$ T cells play critical roles for protection against malaria parasites that can be acquired during natural or experimental infection (1–4). However, the role of CD8$^+$ T cells in protective immunity is controversial. Some studies suggested that CD8$^+$ T cells could transfer protective immunity to an adoptive host (5), whereas others claimed that they did not play a major role in protection against blood stage infection with *Plasmodium* species (6). In contrast, accumulating evidence indicates that CD8$^+$ T cells are involved in the pathogenesis of severe malaria. Cerebral malaria resulting from *Plasmodium falciparum* infection is one of the most severe complications and main cause of death in human malaria (7–11). Using a rodent model of malaria infection with the *Plasmodium berghei* ANKA (PbA)[3] strain, investigations indicated that CD8$^+$ T cells are one of the major effector cells that trigger cerebral malaria. In these experimental models, it was shown that CD8$^+$ T cells were sequestered in the brain during cerebral malaria and that the depletion of CD8$^+$ T cells decreased mortality (8). Furthermore, perforin-mediated killing by CD8$^+$ T cells was required for the pathogenesis of experimental cerebral malaria resulting from PbA infection, suggesting that the effector function of CD8$^+$ T cells is involved in the pathogenesis (9). However, it is unclear whether *Plasmodium*-specific CD8$^+$ T cells are activated during the erythrocyte stage of malaria and how they are involved in the pathogenesis of cerebral malaria.

Because malaria parasites infect RBC that do not themselves express MHC molecules, the infected cells cannot directly present malaria Ags to T cells in association with MHC class I molecules. To activate specific CD8$^+$ T cells, malaria Ags must be presented by a process referred to as cross-presentation by APCs that are themselves not infected, as reported for some minor histocompatibility Ags, tumor Ags, and various pathogens (12, 13). There are two main Ag presentation pathways of cross-presentation; one is the phagosome-to-cytosol pathway that is dependent on the TAP molecule (14), and the other is the TAP-independent pathway in which antigenic peptide is generated and loaded to MHC class I in MHC class II compartments (15) or on the cell surface by peptide regurgitation (16). The former TAP-dependent pathway is used by viruses that do not themselves infect hemopoietic cells (17) or some of the intracellular parasites such as *Mycobacterium tuberculosis* and *Toxoplasma gondii* (18, 19). The latter TAP-independent pathway is used by some pathogen-derived Ags such as those from *Leishmania major* and virus-like particles (20, 21). It is unclear how these different pathways are selected in targeting the exogenous Ags to the MHC class I presentation pathway by each microbial species.

Because class I-restricted Ags have not been identified in malaria parasites during the erythrocyte stage, we used a model Ag OVA to study immune responses of Ag-specific CD8$^+$ T cells

*Division of Immunology, Department of Molecular Microbiology and Immunology, and †Atomic Bomb Disease Institute, Graduate School of Biomedical Sciences, Nagasaki University, Nagasaki, Japan; and ‡Department of Medical Zoology, School of Medicine, Mie University, Tsu, Japan

Received for publication October 19, 2007. Accepted for publication May 13, 2008.

The costs of publication of this article were defrayed in part by the payment of page charges. This article must therefore be hereby marked *advertisement* in accordance with 18 U.S.C. Section 1734 solely to indicate this fact.

[1] This work was supported by Grants-in-Aid from the Ministry of Education, Science, Sports and Culture, Japan; and by the 21c COE program at Nagasaki University.

[2] Address correspondence and reprint requests to Dr. Katsuyuki Yui, Division of Immunology, Department of Molecular Microbiology and Immunology, Graduate School of Biomedical Sciences, Nagasaki University, 1-12-4, Sakamoto, Nagasaki, 852-8523 Japan. E-mail address: katsu@nagasaki-u.ac.jp

[3] Abbreviations used in this paper: PbA, *Plasmodium berghei* ANKA; OVA-PbA, recombinant *Plasmodium berghei* ANKA expressing OVA; WT-PbA, wild-type *Plasmodium berghei* ANKA; hsp, heat shock protein; DHFR-ts, dihydrofolate reductase-thymidyltransferase-ts; KO, knockout; LCMV, lymphocytic choriomeningitis virus; DC, dendritic cell; CD62L, CD62 ligand; OVAp, $OVA_{257-264}$ peptide.

during malaria infection. We generated a recombinant PbA that expresses a cytoplasmic form of OVA (OVA-PbA). Using this system, we show that malaria Ags can be presented to specific $CD8^+$ T cells by cross-presentation in a TAP-dependent manner during the erythrocyte stage of malaria infection and that these activated $CD8^+$ T cells could be pathogenic to the host. Furthermore, $CD8^+$ T cells that are not specific for malaria Ag can be activated during malaria infection in an Ag-nonspecific manner. This activation was at least in part dependent upon the presence of NK cells.

Materials and Methods

Generation of recombinant PbA parasite clones expressing OVA

Recombinant PbA parasites were engineered to constitutively express a truncated C-terminal fragment of OVA (aa 150–386) fused to the N-terminal sequence (aa 1–5) of the PbA heat shock protein (hsp) 70 gene. The gene construct was based on pBluescript KS^+ (Stratagene) and contains the following elements: 1) PbA dihydrofolate reductase-thymidyltransferase-ts (DHFR-ts) gene; 2) PbA hsp70 5′-untranslated region and N-terminal coding sequence; 3) coding sequence of C-terminal fragment of OVA; 4) PbA hsp70 3′-untranslated region and DHFR-ts 3′-untranslated region. The DHFR-ts gene contains a point mutation at position 110 of the DHFR gene causing a Ser→Asn transition conferring resistance to the antimalaria drug pyrimethamine.

The procedure to generate recombinant PbA was described previously (22). In brief, the gene construct was digested with *Sac*I and *Kpn*I to linearize and release the insert from the vector. PbA merozoites were transfected by electroporation and were selected in rats using pyrimethamine. The surviving parasites were further selected by limiting dilution in mice, and parasite clones that were resistant to pyrimethamine were obtained.

Mice, adoptive transfer, and PbA infection

OT-I-transgenic mice expressing the TCR specific for $OVA_{257-264}/K^b$ (23), were provided by Dr. H. Kosaka (Osaka University, Osaka, Japan). TAP knockout (TAP-KO) mice (C57BL/6 (B6) background; Ref. 24) by Dr. H. Watanabe (University of the Ryukyus Okinawa, Japan). B6.SJL-Ptprc congenic (B6.SJL) mice ($CD45.1^+$) by Dr. Y. Takahama (University of Tokushima, Tokushima, Japan), and RAG2 knockout (RAG2-KO) mice (25) by Dr. Y. Yoshikai (Kyushu University, Fukuoka, Japan). TCR P14 lymphocytic choriomeningitis virus (LCMV)/TCRα-KO mice (26) were purchased from Taconic. B6 mice were purchased from SLC. OT-I and B6.SJL mice were bred, and offspring were intercrossed to obtain CD45.1 OT-I mice. RAG2-KO mice and OT-I mice were intercrossed to obtain RAG2-KO OT-I mice. These mice were maintained in the Laboratory Animal Center for Animal Research at Nagasaki University (Nagasaki, Japan) and were used at the age of 8–14 wk. For adoptive transfer, $CD8^+$ T cells (>95%) were purified from CD45.1 OT-I mice using anti-CD8 IMag (BD Biosciences), labeled with CFSE (15 μM; Molecular Probes) and were injected into the tail vein of B6 mice ($0.7–2 \times 10^7$/mice). Mice were infected with WT-PbA or OVA-PbA by i.p. injection of parasitized RBCs (10^4 infected RBC) or by i.v. injection of 10^6 parasitized RBC (Fig. 2*C*). Parasitemia was monitored by microscopic examination of standard blood films, and mice were sacrificed after the parasitemia reached 1.6–18.2% (days 7–9). Brain sequestered lymphocytes were prepared as described (27). Depletion of NK cells was performed by injection of anti-NK1.1 mAb (PK136; 50 μl of ascites fluid partially purified by ammonium sulfate precipitation method) i.p. at −1 day, and i.v. at 2, 5, and 7 days after infection with PbA. The animal experiments reported herein were approved by the Institutional Animal Care and Use Committee of Nagasaki University and were conducted according to the guidelines for Animal Experimentation at Nagasaki University.

Immunoblotting

Peripheral blood cells of PbA-infected mice were washed and then lysed in PBS by freezing and thawing. After centrifugation, lysate (10^7 RBC) was separated on 15% SDS-PAGE and transferred to polyvinylidene difluoride membrane. The blot was blocked and probed with rabbit anti-OVA (Bethyl Laboratories) or rabbit anti-merozoite surface protein 1 Ab. After a washing, the membrane was incubated with HRP-conjugated anti-rabbit Ig Ab, washed, and analyzed using ECL reagents.

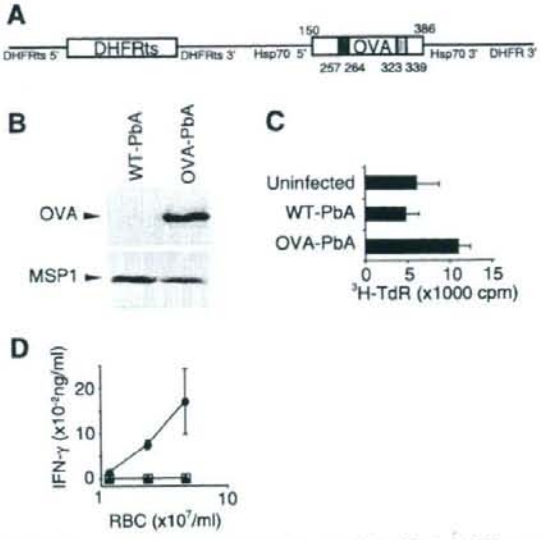

FIGURE 1. The expression of OVA in recombinant PbA. *A*, DNA construct to generate recombinant PbA. The C-terminal OVA coding sequence (aa 150–386) was fused to the N terminus (aa 1–5) of the PbA hsp70 gene. The expression of OVA was controlled by the PbA hsp70 promoter, which is constitutively active during liver and blood stages of the malaria life-cycle. DHFR-ts is a selection marker, which confers resistance to the antimalaria drug pyrimethamine. *B*, The lysates of RBC from B6 mice infected with WT-PbA or OVA-PbA were separated by SDS-PAGE, blotted, and probed with anti-OVA Ab and with anti-merozoite surface protein 1 Ab as control. *C*, OT-I T cells (3×10^5) and splenic DCs ($CD11c^+$ cells, 1×10^4) were cultured in the presence of uninfected freeze-thaw lysates of 9.3×10^6 RBCs or those infected with WT-PbA or OVA-PbA for 2 days, and pulsed for 20 h with [^{3}H]TdR. Parasitemia levels: WT-PbA, 16.9%; OVA-PbA, 18.4%. *D*, OT-I spleen cells (1×10^5) were cultured in the presence of DCs ($CD11c^+$ cells, 3×10^3) and RBCs from uninfected mice (□) or mice infected with WT-PbA (▲) or OVA-PbA (●) for 48 h. The production of IFN-γ in the supernatant was determined by ELISA.

Proliferation and IFN-γ production in vitro

To isolate dendritic cells (DC), B6 spleen was treated with dispase (5 μg/ml; Godo-shusei) for 30 min at 37°C. Spleen cells were treated with anti-CD11c microbeads, and DCs ($CD11c^+$, >90%) were purified using Auto MACS (Miltenyi Biotech). Proliferation of OT-I was determined by culture of OT-I $CD8^+$ T cells (1×10^5) in the presence of DC (3×10^3) and crude RBC Ag (9.3×10^6 RBCs) for 63 h with [^{3}H]TdR for the final 15 h. For IFN-γ assay, OT-I $CD8^+$ T cells (3×10^5) were stimulated with DCs (1×10^4) in the presence of crude malaria Ag (9.3×10^6 RBC) for 48 h, and the levels of IFN-γ in the supernatant were determined by a sandwich ELISA as described previously (28).

Flow cytometry

FcR was blocked with anti-FcγRII/III mAb (BD Biosciences). The staining reagents used in this study include PE-Cy7-anti-CD45.1, allophycocyanin- or PE-anti-CD8, FITC-anti-Vα2, PE- or FITC-anti-CD62 ligand (CD62L), FITC- or biotin-anti-CD44, and PE- or FITC-anti-CD69 mAbs (eBiosciences). $OVA_{257-264}$ H-$2K^b$ tetramer was purchased from MBL. 7-Aminoactinomycin D was added to exclude dead cells from the analysis. For analysis of granzyme B expression, splenocytes were incubated with Fc block and were stained with PE-Cy7-anti-CD45.1 and FITC- or allophycocyanin-anti-CD8 mAbs. Samples were fixed and permeabilized using Cytofix-Cytoperm buffer (BD Biosciences), stained with PE-anti-granzyme B mAb (Caltag), and analyzed using FACSCanto II (BD Biosciences).

Cytotoxicity assay in vitro and in vivo

For in vitro cytotoxicity assay, $CD8^+$ T cells were enriched from spleen cells by $CD8a^+$ T cell isolation kit (Miltenyi Biotech). EL4 target cells

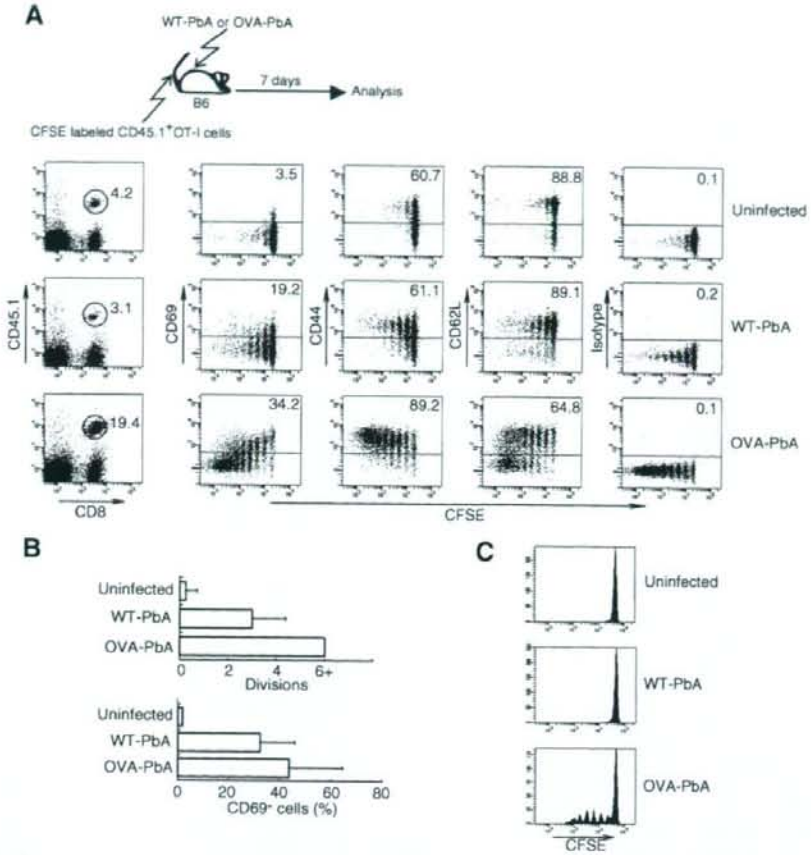

FIGURE 2. Ag-specific and -nonspecific activation of OT-I CD8⁺ T cells in vivo during PbA infection. *A*, CFSE-labeled OT-I CD8⁺ T cells (CD45.1⁺, 8.8×10^6) were adoptively transferred into B6 mice, and the mice were uninfected or infected with WT-PbA or OVA-PbA (1×10^4) i.p. on the same day. Seven days later, spleen cells were stained with allophycocyanin-anti-CD8, PE-Cy7-anti-CD45.1, and PE-anti-activation markers (CD69, CD44, CD62L). Staining profiles of activation markers and CFSE are shown for the CD45.1⁺CD8⁺ gated population. Numbers in the upper right corner indicate percent of cells above the line. Levels of parasitemia: WT-PbA, 10.0%; OVA-PbA, 8.4%. *B*, Summary of cell divisions in the spleen after adoptive transfer of CFSE-CD8⁺ T cells (*top*). Data were obtained from four independent experiments similar to *A*. *Bottom*, Percentage of CD69⁺CD8⁺ T cells obtained from six independent experiments similar to *A* except that transferred OT-I cells were not labeled with CFSE and the staining was performed using FITC-anti-CD69 mAb. In both panels, three groups showed a significant difference in overall comparison ($p < 0.05$; *top*, Savage test; *bottom*, Kruskal-Wallis test); each bar and whisker denote the mean and SD, respectively. The difference in the number of cell divisions was slightly not significant between uninfected and WT-PbA-infected mice ($p = 0.0187$, Savage test), whereas it was significant between uninfected and OVA-PbA-infected mice ($p = 0.0046$), and between WT-PbA-infected and OVA-PbA-infected mice ($p = 0.0047$). The proportion of CD69⁺CD8⁺ T cells was significantly higher in WT-PbA-infected ($p = 0.0025$, Wilcoxon rank-sum test) and OVA-PbA-infected mice ($p = 0.0025$) when compared with uninfected mice, whereas it was not significant ($p = 0.1490$) between WT-PbA-infected and OVA-PbA-infected mice. *C*, CFSE-labeled OT-I CD8⁺ T cells (CD45.1⁺, 1×10^7) were adoptively transferred into B6 mice, which were uninfected or infected with the large dose (1×10^6) of WT-PbA or OVA-PbA i.v. Three days later, spleen cells were analyzed using flow cytometry. Levels of parasitemia: WT-PbA, 1.3%; OVA-PbA, 1.0%.

were labeled with ^{51}Cr with and without $OVA_{257-264}$ peptide (OVAp) for 1 h at 37°C. Target and effector cells were added to each well of a 96-well plate and cultured for 4 h. Percent specific lysis = [(experimental ^{51}Cr release − spontaneous ^{51}Cr release)/(maximum ^{51}Cr release − spontaneous ^{51}Cr release)] × 100. For in vivo cytotoxicity assay, B6 spleen cells were labeled with a high concentration of CFSE (10 μM) and were pulsed with OVAp (1 μg/ml) for 1 h at 37°C or labeled with low concentration of CFSE (1 μM) and were incubated without peptide. Cells from each population were mixed at a 1:1 ratio, and a total of 1×10^7 cells were adoptively transferred into the recipient mice. Mice were sacrificed 4 h later, and spleen cells were analyzed using flow cytometry. Percent specific lysis = [1 − (ratio of peptide-pulsed cells)/(ratio of peptide-unpulsed cells)] × 100.

Evaluation of the disease

Mice were monitored daily after day 5 of infection, and clinical scores were defined by the presence of the typical pathological signs as described (29): level 1, hunching or wobbly; level 2, hunching and wobbly; level 3, hypotonia; level 4, limb paralysis and convulsions; level 5, death.

Statistical analysis

In comparison of three or more groups, overall comparison was first made by ANOVA for one-way or two-way data at the significance level of 0.05, and if significant, each pair of the groups was compared by *t* test. If the ordinary ANOVA was considered to be inappropriate because of the significant departure from normality, censoring in measurements or large variation in the variance among groups, the Kruskal-Wallis test, the Wilcoxon rank-sum test, or the Savage test was used instead with the significance level determined by the Bonferroni procedure controlling the familywise error rate <0.05. For survival data, the log-rank test was used in a similar way. Procedures of ANOVA, LIFETEST, and NPAR1WAY in the SAS system were used for the calculations.

Results

Ag-specific and nonspecific activation of CD8$^+$ T cells during PbA infection

We generated recombinant malaria PbA parasite that constitutively expresses the C-terminal fragment of OVA (aa 150–386) fused to the N terminus of PbA hsp70 (OVA-PbA; Fig. 1*A*). The expression of the recombinant OVA was confirmed by immunoblotting of the infected RBC lysates with anti-OVA Ab (Fig. 1*B*). The ability of DCs to present OVA-PbA Ag was evaluated for proliferation and IFN-γ secretion of OVA-specific OT-I CD8$^+$ T cells in vitro (Fig. 1, *C* and *D*). CD8$^+$ T cells from OT-I mice showed specific proliferation and IFN-γ secretion in response to the DCs pulsed with OVA-PbA-infected RBC. We used adoptive transfer of OT-I CD8$^+$ T cells from TCR-transgenic mice to determine whether Ag-specific CD8$^+$ T cells can be primed during PbA infection. B6 mice (CD45.2$^+$) were adoptively transferred with CFSE-labeled OT-I CD8$^+$ T cells (CD45.1$^+$) and were infected with wild-type *P. berghei* ANKA (WT-PbA) or OVA-PbA. The proliferation of OT-I CD8$^+$ T cells was monitored by the sequential loss of CFSE intensity 7 days after infection (Fig. 2, *A* and *B*). The proportion of OT-I CD8$^+$ T cells increased in mice infected with OVA-PbA (19.4%) when compared with uninfected mice (4.2%) or mice infected with WT-PbA (3.1%). OT-I CD8$^+$ T cells divided minimally and remained CD69$^-$CD44^{low}CD62L^{high} in the uninfected host. Extensive division of OT-I CD8$^+$ T cells was observed in mice infected with OVA-PbA. In addition, up-regulation of the CD69 marker was observed in cells that divided 0–3 times, and up-regulation of CD44 and down-regulation of CD62L were evident in cells that have divided multiple times, indicating that OT-I CD8$^+$ T cells were activated in an Ag-specific manner during infection with PbA. Unexpectedly, OT-I CD8$^+$ T cells divided ~4 times and up-regulated the CD69 marker in mice infected with WT-PbA, suggesting that OT-I CD8$^+$ T cells can be activated in an Ag-nonspecific manner during infection with WT-PbA. Because it was recently reported that malaria infection impairs cross-presentation (30), we examined the ability of host APC to present OVA-PbA Ag during early (days 0–3) and late (days 5–8) periods after infection (Figs. 2*C* and 4*A*, *left*). In both periods, OT-I cells proliferated several times in vivo after infection with OVA-PbA but not with WT-PbA, indicating that APC can cross-present malaria Ag throughout infection with PbA.

We have also analyzed lymphocytes in the brain. The number of CD8$^+$ T cells retained within the brain was increased in mice infected with WT-PbA or OVA-PbA (Fig. 3*A*). A large variation in the number of CD8$^+$ T cells in the infected mice might reflect their differential stages of cerebral malaria. OT-I cells, however, were increased only in mice infected with OVA-PbA. The number of CD4$^+$ T cells was not significantly different between these groups of mice. We also examine the CFSE profile and surface phenotype of OT-I cells that were sequestered in the brain (Fig. 3*B*). OT-I cells in the brain of OVA-PbA-infected mice uniformly showed low levels of CFSE and CD44^{high}CD62L^{low} phenotype, indicating that only highly activated OT-I cells were retained within the brain of mice infected with OVA-PbA.

Activation of malaria-specific CD8$^+$ T cells is TAP dependent

To determine whether the Ag presentation of OVA epitope to OT-I CD8$^+$ T cells utilize the conventional class I Ag presentation pathway, we examined the requirement for the TAP molecule in proliferation of OT-I CD8$^+$ T cells in vivo in TAP null mice (TAP-KO; Fig. 4, *A* and *C*). In this experimental system, we monitored the T cell response in vivo within 3 days after transfer, given that the number of OT-I CD8$^+$ T cells was severely reduced 5 days after transfer, perhaps due to their rejection in TAP-KO host mice (data not shown). Thus, we infected B6 or TAP-KO mice with WT-PbA or OVA-PbA, adoptively transferred CFSE-labeled CD8$^+$ T cells from CD45.1$^+$OT-I mice 5 days later, and monitored proliferation of OT-I T cells by the sequential loss of CFSE intensity 3 days later (parasitemia 2.3–5.4%). Division of OT-I cells was not detectable in uninfected or WT-PbA-infected hosts during these 3 days. In B6 mice infected with OVA-PbA, however, OT-I cells divided several times, indicating that they were activated in vivo in an Ag-specific manner. In TAP-KO hosts, no proliferative responses were observed, indicating that Ag presentation of the OVA epitope expressed in OVA-PbA in association with the MHC class I molecule, was dependent on the TAP molecule. However, OT-I CD8$^+$ T cells showed increased expression of CD69 and reduced expression of CD62L in the TAP-KO host mice infected with WT-PbA or OVA-PbA, suggesting that these phenotypical changes of OT-I CD8$^+$ T

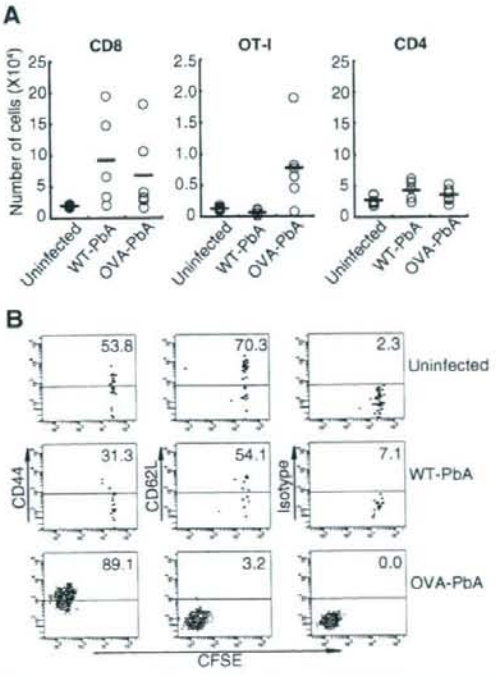

FIGURE 3. Sequestration of T cells in the brain of mice infected with PbA. *A*, B6 mice were adoptively transferred with OT-I CD8$^+$ T cells (CD45.1$^+$) and were uninfected or infected with WT-PbA or OVA-PbA. After elevation of parasitemia (WT-PbA, 2.2–12.9%; OVA-PbA, 1.2–8.4%), lymphocytes in the brain were collected and stained with allophycocyanin-anti-CD8, PE-anti-CD4, and PE-Cy7-anti-CD45.1 mAb. The numbers of T cell subsets were determined by multiplying the total number of cells with the percentage of each population. Overall comparison showed a significant difference both in the number of CD8$^+$ T cells and in OT-I ($p < 0.05$, Kruskal-Wallis). However, the difference in the former was slightly not significant between uninfected and WT-PbA-infected mice ($p = 0.0179$, Wilcoxon rank-sum test) and between uninfected and OVA-PbA-infected mice ($p = 0.0328$), whereas in the latter the difference was significant between OVA-PbA-infected mice and WT-PbA-infected mice ($p = 0.0112$) and was slightly not significant between OVA-PbA-infected mice and uninfected mice ($p = 0.0328$). Overall comparison of the number of CD4 showed no significant difference ($p = 0.1394$, Kruskal-Wallis test). *B*, CFSE-labeled OT-I CD8$^+$ T cells (CD45.1$^+$) were adoptively transferred into B6 mice, which were uninfected or infected with WT- or OVA-PbA. Brain lymphocytes were stained with mAbs as described in Fig. 2*A*. Staining profiles of activation markers and CFSE are shown for the CD45.1$^+$CD8$^+$ gated populations. Numbers in the upper right corner indicate percentage of cells above the line. Levels of parasitemia: WT-PbA, 10.1%; OVA-PbA, 9.4%. Representative data of two similar results are shown.

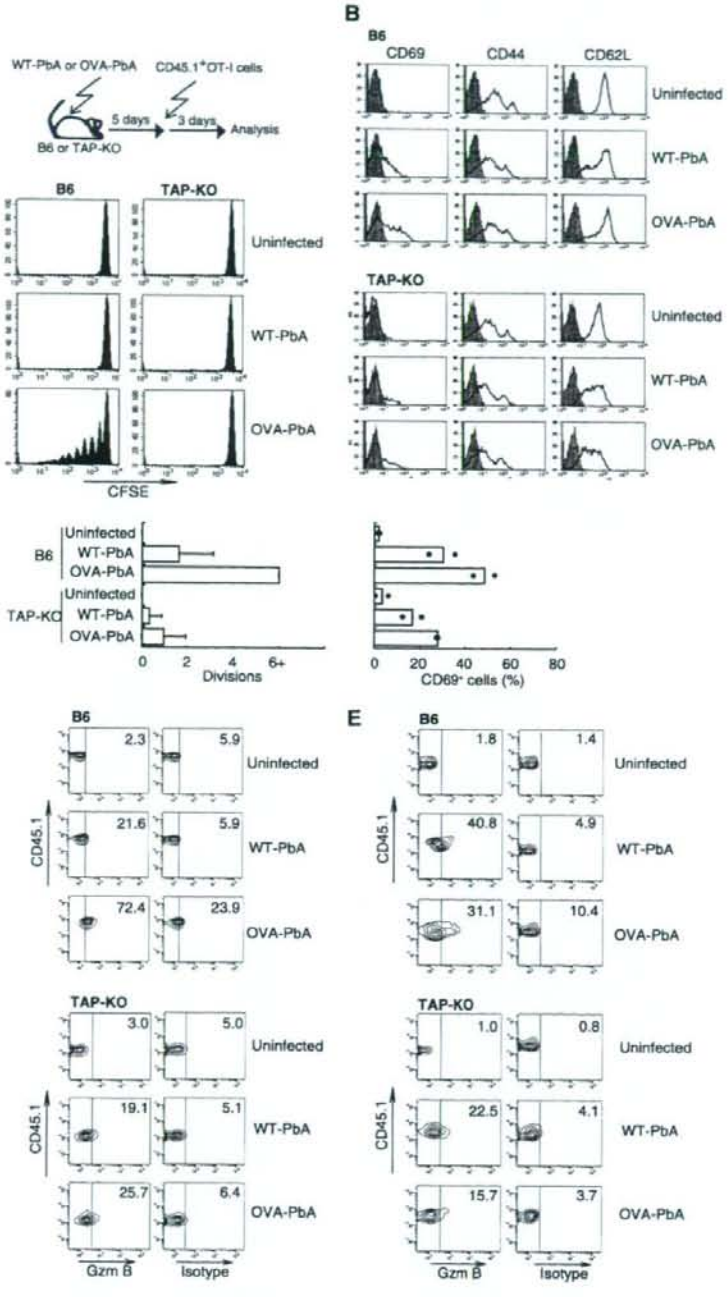

FIGURE 4. Specific activation of OT-I $CD8^+$ T cells during infection with OVA-PbA is TAP dependent. B6 or TAP-KO mice were uninfected or infected with WT-PbA or OVA-PbA. Five days later, mice were inoculated with CFSE-labeled $CD8^+$ T cells (1×10^7 in *A*, 2×10^7 in *B*) from CD45.1$^+$OT-I mice. Three days later, spleen cells were stained with allophycocyanin-anti-CD8, with PE-Cy7-anti-CD45.1 (*A*), or with additional FITC-antiactivation marker mAbs (CD69, CD44, CD62L) (*B*). The CFSE profiles (*A*) or staining profiles of activation markers (solid line) and isotype control (dark histogram) (*B*) of the CD45.1$^+$$CD8^+$ gated populations are shown. *C*, Summary of the cell divisions ($n = 3$) and CD69$^+$ cells ($n = 2$; each dot represents the result of one mouse) performed as in *A* and *B*. In B6 mice, a significant difference was observed in overall comparison of the number of cell divisions among three groups of mice ($p < 0.05$, Savage test), whereas no such difference was observed in TAP-KO mice. In B6 mice, the number of cell division was significantly larger in OVA-PbA-infected mice compared with WT-PbA-infected mice ($p = 0.0143$, Savage test) and uninfected mice ($p = 0.0127$), while the difference was not significant between WT-PbA-infected and uninfected ($p = 0.0732$); each bar and whisker denote the mean and SD, respectively. *D* and *E*, Staining profiles of the CD45.1$^+$$CD8^+$ gated populations of spleen cells prepared as in *B*, stained with allophycocyanin-anti-CD8, PE-Cy7-anti-CD45.1, and PE-anti-granzyme B (Gzm B) mAbs or PE-isotype control ex vivo before (*D*) and after culture on plates coated with anti-TCR mAb for 5 h (*E*). The number in each panel indicates the percentage of positive cells. The high background of the isotype control (23.9%) was observed without PE-isotype Ab, suggesting that it was due to autofluorescence. Levels of parasitemia in WT-PbA (3.2–5.4%) and OVA-PbA (2.4–6.1%)-infected B6 mice: WT-PbA (2.3–6.2%)-infected mice; and OVA-PbA (4.7–5.5%)-infected TAP-KO mice.

cells could be induced without TCR occupancy during PbA infection (Fig. 4, *B* and *C*). We also evaluated their expression of granzyme B by intracellular staining in this model. The expression of granzyme B was undetectable in OT-I $CD8^+$ T cells in uninfected mice but was detected in OT-I $CD8^+$ T cells in WT-PbA or OVA-PbA-infected mice both before and after culture (Fig. 4, *D* and *E*). The level of granzyme B expression in OT-I $CD8^+$ T cells ex vivo was higher in OVA-PbA-infected mice than in WT-PbA-infected mice. OT-I $CD8^+$ T cells transferred into TAP-KO mice also showed up-regulation of granzyme B expression, suggesting that it could be induced without TCR occupancy during malaria infection.

Involvement of NK cells in nonspecific activation of $CD8^+$ T cells

It has been reported that NK cells are activated during malaria infection and play pivotal roles in the induction and recruitment of specific $CD8^+$ T cells (31–33). To examine whether $CD4^+$ T

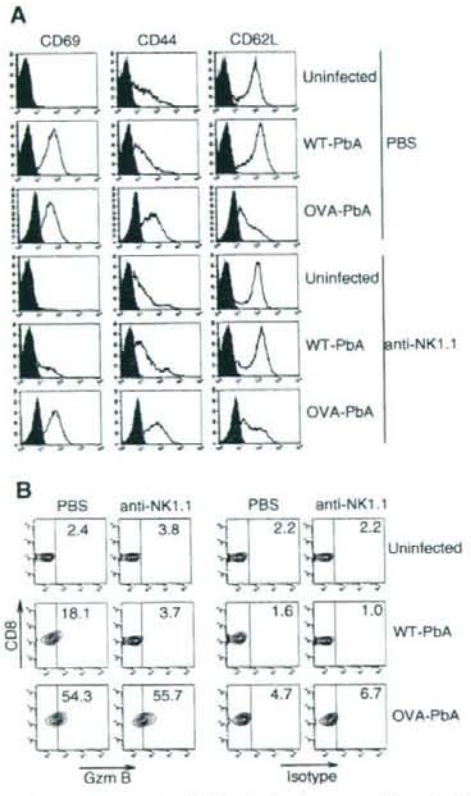

FIGURE 5. Involvement of NK cells in the nonspecific activation of OT-I CD8$^+$ T cells during infection with PbA. RAG2-KO OT-I mice were inoculated with PBS or anti-NK1.1 mAb on −1, 2, 5, and 7 days after infection with WT-PbA or OVA-PbA. On day 8, spleen cells were stained with PE-anti-CD8 and FITC-labeled activation markers (CD69, CD62L, CD44; solid line; *A*), or with FITC-anti-CD8 and PE-anti-granzyme B (Gzm B; *B*). Data represent staining profiles of CD8$^+$-gated populations. Levels of parasitemia: WT-PbA, PBS-treated (6.5%), NK-depleted (5.4%); OVA-PbA, PBS-treated (18.2%), NK-depleted (14.2%). Values are representative data of two similar results.

cells, other CD8$^+$ T cells, or NK cells are involved in the activation of OT-I CD8$^+$ T cells, we infected RAG2-KO OT-I mice, which lack an adaptive immune system except for monoclonal OVA-specific OT-I CD8$^+$ T cells, with PbA. OT-I CD8$^+$ T cells showed clear up-regulation of the CD69 marker in mice infected with WT-PbA or OVA-PbA, indicating that OT-I CD8$^+$ T cells did not require CD4$^+$ T cells or other CD8$^+$ T cells for their activation (Fig. 5*A*). The expression of granzyme B was also detected in OT-I CD8$^+$ T cells in RAG2-KO OT-I mice that were infected with WT-PbA or OVA-PbA, indicating that the help of CD4$^+$ T cells or other CD8$^+$ T cells was not required for the induction of granzyme B (Fig. 5*B*). When NK cells were depleted by treatment with anti-NK1.1 mAb in vivo, up-regulation of CD69 and the expression of granzyme B were severely impaired in CD8$^+$ T cells from WT-PbA-infected mice (Fig. 5). OT-I CD8$^+$ T cells, however, were activated in NK1.1-treated OVA-PbA-infected mice at levels indistinguishable from the control group, indicating that NK cells are not required for Ag-specific activation of CD8$^+$ T cells during blood stage infection with PbA. It was reported that NK markers are expressed in T cells of virus-infected

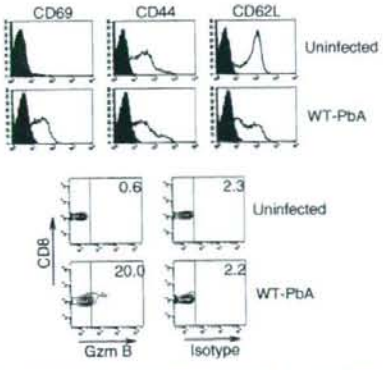

FIGURE 6. Nonspecific activation of CD8$^+$ T cells from P14 TCR-transgenic mice. Eight days after infection with WT-PbA, spleen cells from P14 mice were stained with anti-CD8 and FITC-labeled activation markers (CD69, CD62L, CD44) or PE-anti-granzyme B (Gzm B). Data represent staining profiles of CD69, CD62L, and CD44 (solid line) and granzyme B of CD8$^+$-gated populations. The level of parasitemia was 15.7%.

mice (34). In RAG2-KO OT-I mice, ~14 and 21% of CD69$^+$CD8$^+$ T cells became NK1.1$^+$ during infection with WT-PbA and OVA-PbA, respectively (data not shown). Therefore, the effect of NK1.1 mAb on WT-PbA-infected mice was not simply due to the direct depletion of activated CD8$^+$ T cells. In addition, the reduction of the activated OT-I CD8$^+$ T cells was seen in WT-PbA-infected mice and not in OVA-PbA-infected mice. Taken together, these results suggested that NK cells were involved in Ag-nonspecific activation of CD8$^+$ T cells during PbA infection.

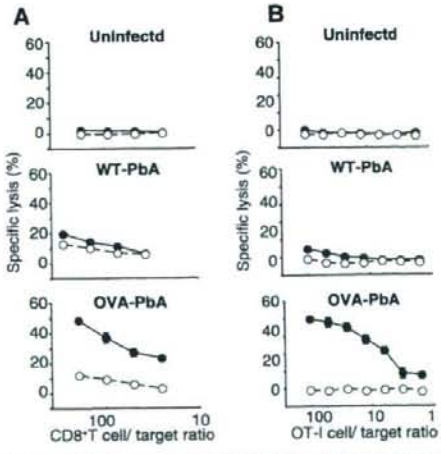

FIGURE 7. CTL activity in vitro of CD8$^+$ T cells during PbA-infection. *A*, B6 mice were uninfected or infected with WT-PbA or OVA-PbA. Five days later, mice were inoculated with CD8$^+$ T cells (1.1×10^7) from CD45.1$^+$OT-I mice. Three days later, CD8$^+$ T cells were purified by negative selection (>83%) and were subjected to ^{51}Cr release assay using OVAp-pulsed (1 μg/ml; ●) and unpulsed (○) EL4 targets for 4 h. Proportions of OT-I cells in CD8$^+$ T cells: uninfected, 8.0%; WT-PbA, 11.0%; OVA-PbA, 31.1%. Levels of parasitemia: WT-PbA, 3.4%; OVA-PbA, 4.0%. *B*, RAG2-KO OT-I mice were infected with WT-PbA or OVA-PbA. Eight days later, purified CD8$^+$T cells were subjected to ^{51}Cr release assay as in *A*. The number of OT-I cells in CD8$^+$T cells was determined based on the percent of OVAp/H-2K^b tetramer-positive cells. Levels of parasitemia: WT-PbA, 5.9%; OVA-PbA, 5.6%.